SKB

TECHNICAL REPORT 93-15

Analysis of the regional groundwater flow in the Finnsjön area

Anders Boghammar, Bertil Grundfelt, Hans Widén

Kemakta Konsult AB

June 1993

SVENSK KÄRNBRÄNSLEHANTERING AB
SWEDISH NUCLEAR FUEL AND WASTE MANAGEMENT CO
BOX 5864 S-102 48 STOCKHOLM
TEL 08-665 28 00 TELEX 13108 SKB S
TELEFAX 08-661 57 19

ANALYSIS OF THE REGIONAL GROUNDWATER FLOW IN THE FINNSJÖN AREA

Anders Boghammar, Bertil Grundfelt, Hans Widén

Kemakta Konsult AB

June 1993

KEMAKTA AR 93-12

Analysis of the regional groundwater flow in the Finnsjön area

Anders Boghammar
Bertil Grundfelt
Hans Widén

KEMAKTA Konsult AB

June, 1993

Keywords: Groundwater flow, regional hydrology modelling, Geographical Information System, Finnsjön

Abstract (English)

The present study on regional groundwater flow in the Finnsjön area was performed by Kemakta Consultant Co. under contract from the Swedish Nuclear Fuel and Waste Management Company (SKB). The study was initiated by the discussions following the SKB 91 study. In the present report, the large scale regional groundwater flow situation in a vertical cross section through the Finnsjön site is analysed using two-dimensional finite-element modelling assuming the rock can be described as a porous media.

The analysis is focused on the effect of the position of the upstream lateral boundary and to what degree different fracture zone patterns influence the flow situation around the area that was used as an example repository site in SKB 91. It is of special interest to investigate if any of the chosen variations can result in an upward flow of water in the repository area with shorter groundwater travel times as a consequence.

The potential effects of the following were studied:

- three different sizes of the modelled domain: 43 km, 26 km and 18 km,
- a number of different generic fracture zone patterns and
- a number of different combinations of rock matrix and fracture zone hydraulic conductivity.

In all, 19 model cases were performed.

The modelling was performed using the finite element code NAMMU together with the program package HYPAC for pre- and post processing. Topographical data for the region were taken from the SKB GIS database.

Stockholm, June, 1993

Abstract (Swedish)

Denna studie rörande regional grundvattenströmning i Finnsjöområdet har utförts av Kemakta Konsult AB på uppdrag av Svensk Kärnbränslehantering AB (SKB). Studien har sitt ursprung i diskussionerna efter SKB 91. I föreliggande studie har grundvattenflödet i ett vertikalt snitt genom Finnsjöområdet studerats enligt finita-element metoden med användning av poröst medium-approximationen.

Studien har i huvudsak inriktats på att undersöka effekten av olika positioner för modellens uppströmsrand samt till vilken grad olika sprickzonsmönster påverkar vattenflödet i det område som valdes som förvarsplats i SKB 91. Det var av särskilt intresse att undersöka om några av de genomförda modellvariationerna kunde ge en uppåtriktad vattenströmning i förvarsområdet och därmed resultera i förkortade transportvägar och gångtider för vattnet.

Följande variationer har studerats:

- Tre olika storlekar på modellområde: 43 km, 26 km och 18 km,
- ett antal olika generiska sprickzonsmönster och ett antal olika kombinationer av hydraulisk konduktivitet i berg och sprickzoner samt
- ett antal beräkningar utan flacka och/eller branta sprickzoner.

Totalt 19 beräkningsfall har genomförts.

Modelleringen har utförts med hjälp av finita-elementmetoden med datorprogrammet NAMMU tillsammans med programpaketet HYPAC för för- och efterbearbetning. Topografiska data för regionen har hämtats från SKB:s GIS-databas.

Stockholm, juni, 1993

Table of contents

1 Introduction

The present project comprises an analysis of the regional groundwater flow at the Finnsjön site used in the SKB 91 performance assessment project [*SKB, 1992*]. Within SKB 91 a series of deterministic groundwater flow calculations were performed [*Lindbom and Boghammar, 1992*]. The main objective of these calculations was to form a reference case for the far-field flow analysis within the project. The results from these calculations were used as boundary conditions for stochastic continuum simulation of the groundwater flow in the Finnsjön area using the HYDRASTAR code [*SKB, 1993*].

After the SKB 91 safety assessment was completed there has been some criticism concerning the groundwater modelling of the Finnsjön area (e.g. [*SKI, 1992*]). One of the points that have been raised is to what degree the extent of the chosen modelling domain influenced the groundwater flow in the repository area. It was stated in the criticism that the SKB 91 analysis was lacking an analysis of the uncertainty from important hydrological factors and how these uncertainties could affect the calculated results. Especially the upstream boundary was regarded to be located too close to the area of interest. It was expressed that the repository may not lie within an infiltration area and that regional groundwater movements caused by features outside the modelled domain could reverse the calculated downward flow at repository depth.

In order to address the criticism, it was decided by SKB that regional two-dimensional groundwater modelling should be performed to investigate the effect of the position of the upstream lateral boundary and to what degree different fracture zone patterns influence the flow situation around the area that was used as an example repository site in SKB 91. The terms regional model and regional effects are used in this report for horizontal extensions of more than 3 km from the repository, and consequently, local scale refers to distances of less than 3 km. It is of special interest to investigate if any of the chosen variations can result in an upward flow of water in the repository area with shorter groundwater travel times as a consequence.

Regional groundwater modelling will be a part of future site selection procedure. This study is useful as a test of methods for initial geohydrologic analysis that might be applied in the forthcoming site investigations.

A database based on a GIS (Geographical Information System) program is currently under development at SKB. This database stores various kinds of geographical data, such as ground surface elevation and geological maps. In previous work [*Boghammar, 1993*] the technique of using topography data obtained from the SKB GIS-database as input to groundwater flow modelling has been developed. The conclusion from this work was that in large-scale models, and given the geohydrological conditions of Sweden, it is reasonable that the groundwater level follows the topography. Furthermore, this method of combining GIS with HYPAC [*Kemakta, 1993*] and NAMMU [*Hartley and Jackson, 1992*] is a very convenient way of working, especially when there is reason to apply detailed topography data to large-scale models.

2 Model description

2.1 General

The present study is an analysis of the influence of the following set of characteristics on the regional groundwater flow at the Finnsjön site:

- Location of upstream boundary.
- Fracture zone geometries.
- Permeability contrast between fracture zones and rock mass.
- Depth dependency of hydraulic conductivity.

2.2 Basic assumptions

In order to be able to carry out a large number of calculations with changing conditions, it was decided that the model should be two-dimensional and that all calculations should be deterministic using the finite-element code NAMMU [*Hartley and Jackson, 1992*]. No modelling of transient flow has been performed although the presence of deep saline water in the Finnsjön area could justify calculation of time-dependent flow including salt transport and consequent density variations. Although it has been stated in [*Voss and Andersson, 1991*] that "During the period of land-rise, the variable density of fluids in the upper few kilometers of bedrock has little effect in the regional flow behavior", it cannot be precluded how density variations from salt gradients can affect the flow at the repository location.

All calculations are made for the same cross-section, the so called A–A'-section, that also was used as an evaluation section in SKB 91. Vertical fracture zones are placed in the models at the surface positions on lineament maps of the known fracture zones and are assumed to dip 90° with an extension down to the bottom boundary of the model. Subhorizontal zones are constructed in generic patterns as described below in Section 2.4.2. Topography from the SKB GIS-database along the A–A'-section with a resolution of 500 m lateral grid and an accuracy of ±2.5 m has been used as input data for the generation of the surface boundary. An interpolation was made to obtain topography data on 50 m intervals. The interpolation was performed by Odin [*1993*].

All model boundaries, except the surface, are assigned a no-flow boundary condition.

2.3 Model geometry

2.3.1 Location of upstream boundary

The two-dimensional model generated is located along the A–A'-section defined in the SKB 91 project [*SKB, 1992*]. Figure 2.1 shows a part of northern Uppland with the Finnsjön area and the location of the A–A'-section. Vertical fracture zones included in the model is indicated with gray dots and numbered from 1 to 9, see Section 2.4.1.

Figure 2.2 is a raster image obtained from the SKB GIS-database representing the ground surface elevation.

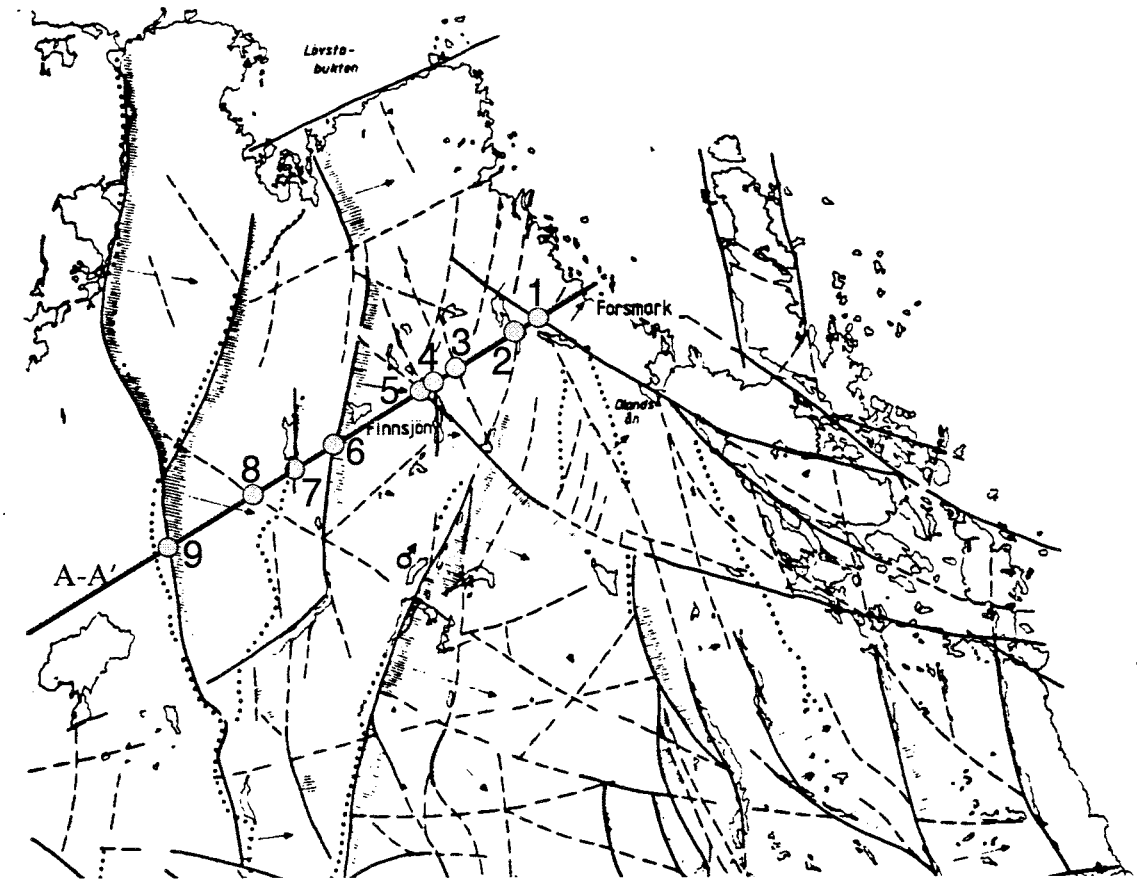

Figure 2.1 *Lineament map of northern Uppland with the Finnsjön area. Location of A-A' and fracture zones [Ahlbom, et al., 1987]. The circles 1-9 indicate the intersection between the modelled cross section and assumed vertical fracture zones.*

Section A–A' was chosen as modelling section for the present study because it is roughly aligned with the main topographical gradient in the area. It cuts through the repository area and several major lineaments. In addition to this, aligning the two-dimensional model to the A–A'-section made comparisons with results from SKB 91 possible. Another reason for choosing the A–A'-section is that the influence of the regional topography would likely be smaller in the repository area if another section, e.g. section 4, from SKB 91 had been selected instead.

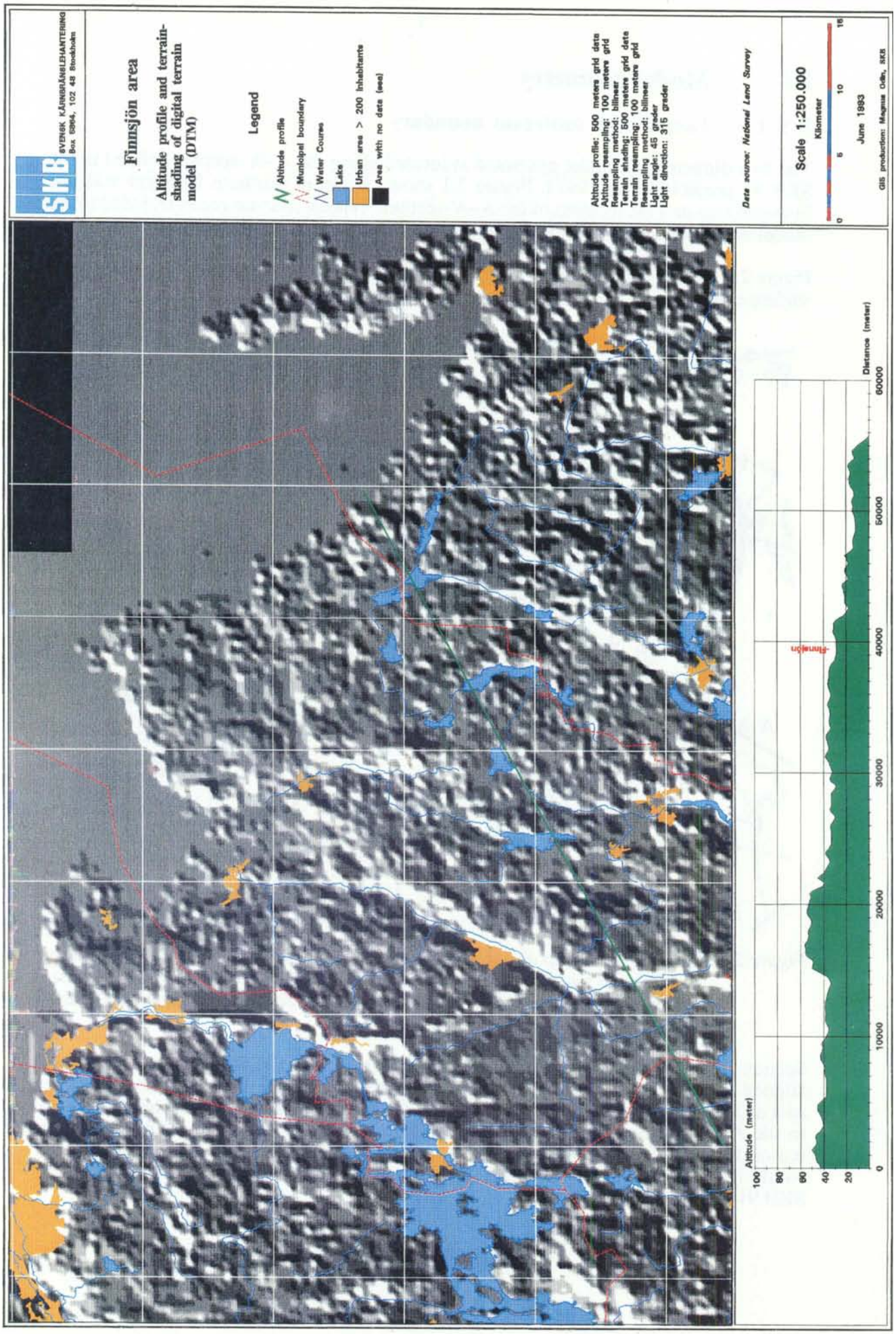

Figure 2.2 *Raster image of the topography of the Finnsjön area. Note that the scaling of the x-axis is reversed compared to all other figures in this report.*

Figure 2.3 shows the area modelled in the SKB 91 project. Note that the intersection of the A-A'-section and the HYDRASTAR block is about 3000 m long whereas the intersection with the repository is only about 200 m long. The intersection with the HYDRASTAR block is used for the starting locations for the pathlines, see Chapter 3.

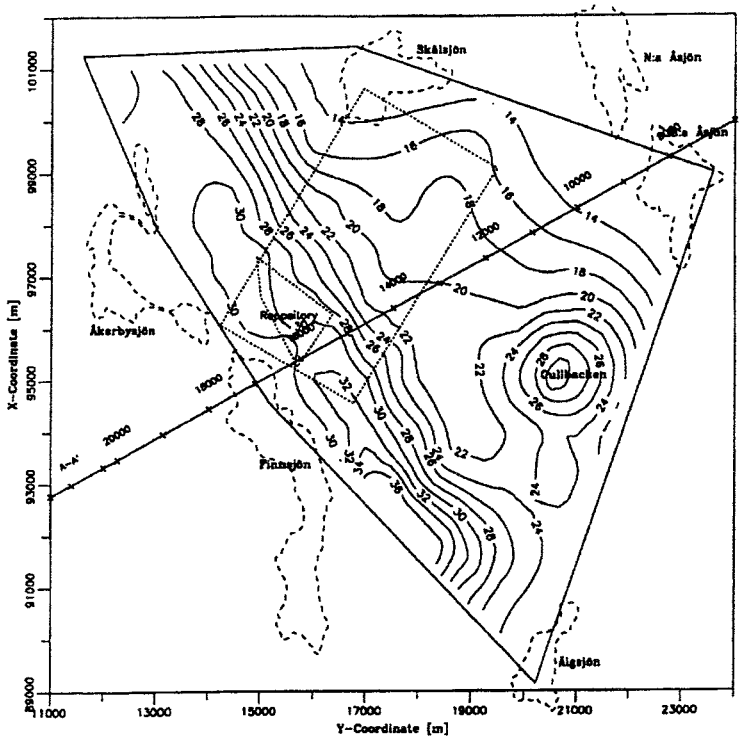

Figure 2.3 *Location of the two-dimensional model within the SKB 91 modelling area. The numbers along the A–A'-line indicate the x-coordinate in the two-dimensional model used in the present study.*

In order to investigate the effect of varying the position of the upstream boundary, three different model regions called R1, R2 and R3 were studied. All three models end at a vertical fracture zone (including the zone). Variations in model dimensions are shown in Table 2.1. The R1 boundary is roughly coinciding with the boundary that was used in SKB 91. The R2 and R3 boundaries are located further upstream at the intersections with fracture zones that are shown on the lineament map in Figure 2.1. The position of these fracture zones were measured from the lineament map and were not fine-tuned to match the topography data. The positions of the upstream boundaries are shown in Figure 2.4.

Table 2.1 *Variations of model domain size. The "zone no." column indicates the bounding fracture zone for the upstream boundary with numbering according to Figure 2.1.*

Model	Xmin [m]	Xmax [m]	Zmin [m]	Zmax [m]	Zone no.
R3S	0	42890	-3000	57	9
R2S	0	26146	-3000	40	6
R1S	0	17775	-3000	35	5

2.3.2 Topography

The topography used was obtained from the SKB GIS-database (Geographical Information System) currently during development. The database used describes the topography on a 500 m grid and was obtained from the National Land Survey [*Odin, 1993*]. The elevation accuracy is ±2.5 m. This database was thereafter interpolated into a 50 m grid along the A–A'- section. Data was obtained from the Baltic sea, at 0 meter, and 57 km inland. The maximum elevation in the area is 57 m above sea level. Figure 2.4 shows the topography that was used. Indicated in Figure 2.4 is also the extension of the three models used, see Section 2.3.1. Note the exaggerated scale on the altitude axis.

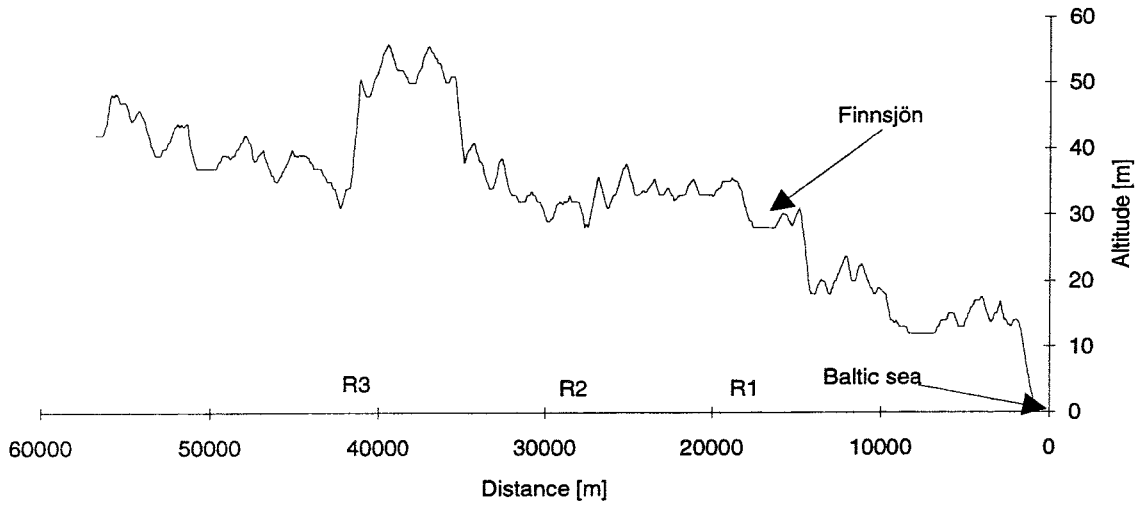

Figure 2.4 *Topography extracted from the SKB GIS-system. R1-R3 denote the location of the alternative locations of the upstream boundary.*

2.4 Hydrological features

2.4.1 Vertical fracture zones

Vertical fracture zones have been included in the model at the location according to the map in Figure 2.1. Since this is a generic, large-scale study, the locations of these vertical fracture zones have not been established with high precision. Therefore the repository and Finnsjön locations in Figure 2.3 may not exactly coincide with the location in the figures in the result presentation in this new study. Table 2.2 describes the vertical fractures. All vertical fracture zones are assumed to have a 90° dip and extend to the bottom boundary of the model.

Table 2.2 Vertical fracture zones.

Name	Distance from shore [m]	Width [m]	Corresponding feature in the SKB 91 study
1	5681	100	
2	8007	100	Dannemora
3	13588	100	Imundbo
4	15913	50	Zone 14
5	17775	100	
6	26146	100	
7	30332	100	
8	34984	50	
9	42890	100	

2.4.2 Subhorizontal fracture zones

A number of different geologic conceptual models have been evaluated in this study. This is performed in order to visualize how the groundwater flow patterns in the repository area is affected by the conceptual uncertainty regarding structural patterns. Although, borehole data exist only for the upper few hundreds of metres, it is reasonable to assume that gently dipping fracture zones exist frequently down to several km depth at the Finnsjön site and its surrounding region. This spacing was also partly applied in SKB 91 for gently dipping zones. Data from Finnsjön and SFR suggest that for gently dipping zones both a westerly (e.g. Zone 2 from SKB 91 [*SKB, 1992*]) and an easterly dip (e.g. Zone H2 in SFR [*SKB, 1987*]) of 10-20° could be assumed. A more detailed description of the assumptions concerning the fracture zone patterns is found in Appendix B.

The generic fracture zone patterns were generated with a vertical spacing of 600 m between subhorizontal fracture zones having a dip of either +15° or -15°. The fracture zones extend only between vertical fracture zones, except for two of the fracture patterns (pattern 4 and 5) where one horizontal fracture zone continue through all vertical fracture zones.

Five different generic fracture patterns have been generated. In fracture pattern 1, horizontal fracture zones on opposite sides of a vertical fracture zone are displaced by 100 metres. In fracture pattern 2 there is no such displacement.

In fracture pattern 3 there are zones dipping both +15° and -15° between two vertical fracture zones. In fracture pattern 4 and 5 a subhorizontal fracture zone extending over the entire length of the model was added to fracture pattern 1. The two patterns including the extended subhorizontal fracture zones that continue through all vertical zones have been included as "worst case" scenarios. There is no indication that fracture zones with such large extension are present in the Finnsjön area or at other sites. In fact the generally accepted view on subhorizontal fracture zones is that they are likely to be interrupted at the vertical fracture zones.These two fracture zone patterns were modelled to investigate the possible consequences if that type of regional structures would exist. In pattern 4 it has a dip of +5° and in fracture pattern 5, a dip of -5°.

All fracture patterns were generated using the location of Zone 2 in the A–A'-section as a reference. The extended fracture zones in pattern 4 and 5 is positioned at 700 m depth between the two vertical fracture zones enclosing the repository. A schematic picture of fracture pattern 1 is shown in Figure 2.5 and fracture pattern 3 is shown in Figure 2.6. In Figure 2.7 the logarithm of the hydraulic conductivity assigned for all five fracture patterns have been plotted.

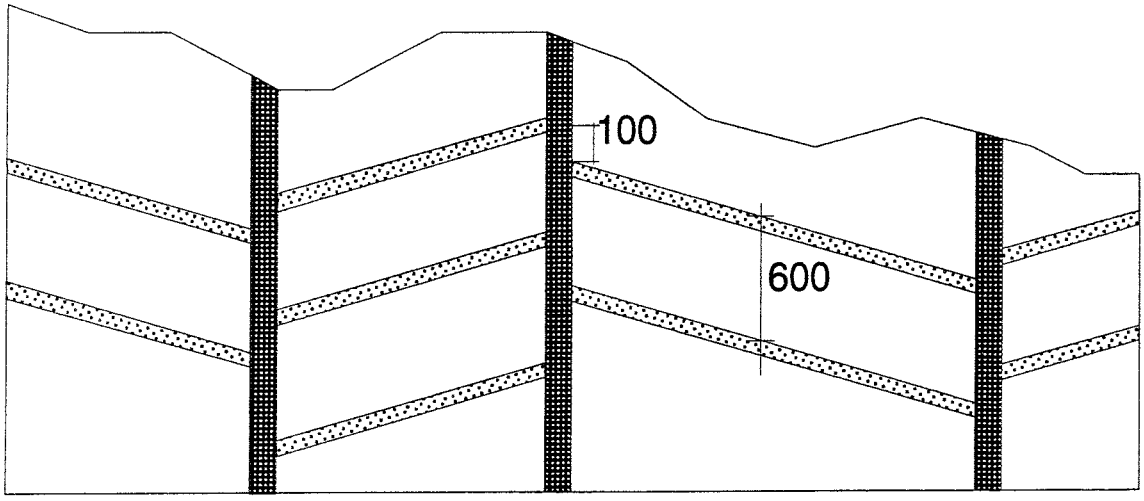

Figure 2.5 Schematic picture of fracture pattern number 1.

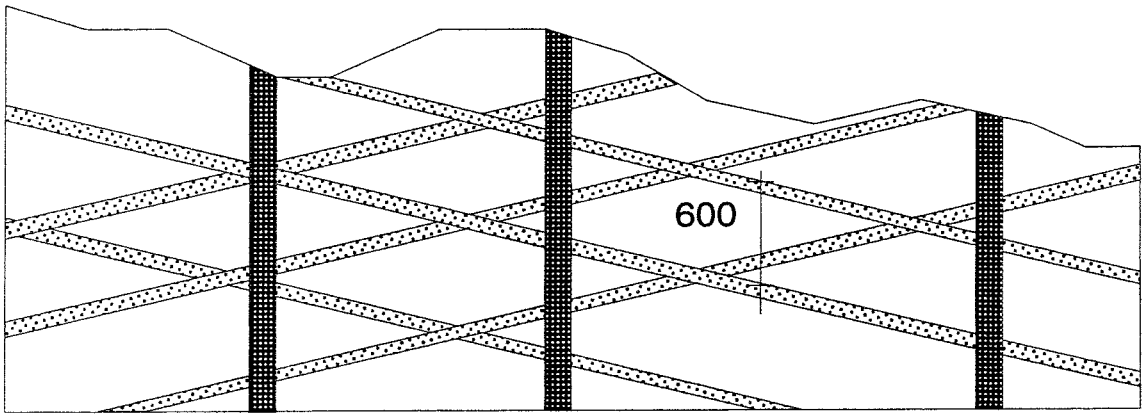

Figure 2.6 Schematic picture of fracture pattern number 3.

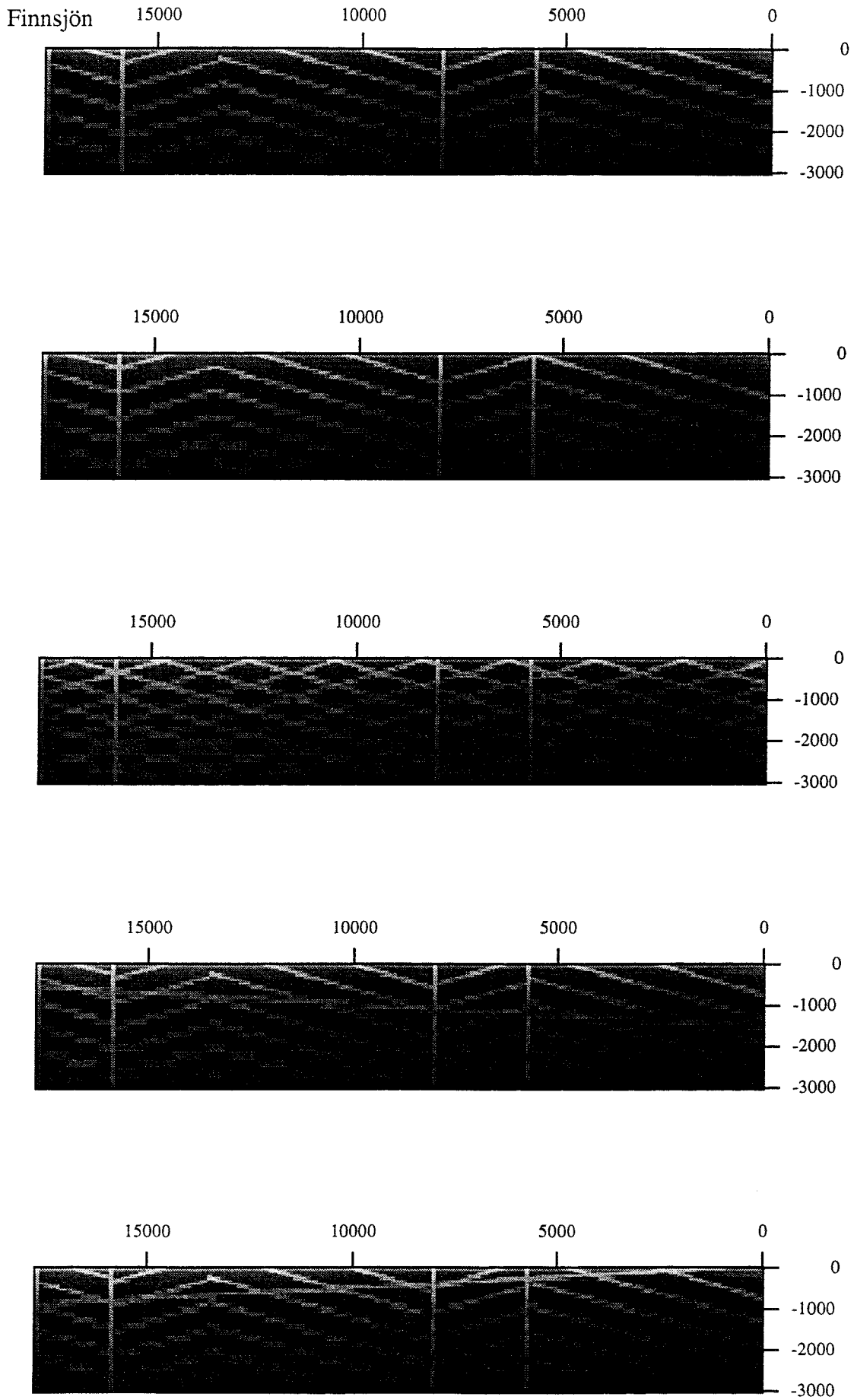

Figure 2.7 *Plots of the hydraulic conductivity as assigned for the five fracture patterns for model domain R1. Pattern 1 at the top and pattern 5 at the bottom of the page.*

2.4.3 Hydraulic conductivities

The assigned hydraulic conductivities are listed in Table 2.3. The depth dependency function used is the same as was used in SKB 91.

Table 2.3 Hydraulic conductivities used in this study. RM=Rock-Mass conductivity.

Description	Rock mass	Vertical zones	Horizontal zones	Extended zones
Homogenous	†	1·RM	1·RM	
Rock mass depth dependent	$1.2 \cdot 10^{-2} \cdot d^{-2.23}$ (d = depth)	‡	‡	
Constant rock mass	$1 \cdot 10^{-8}$	‡	‡	
High contrast	†	100·RM	1000·RM	
Large contrast	†	100·RM	100·RM	
Small contrast	†	4.5·RM	10·RM	
Vertical fracture zones only	†	100·RM	1·RM	
Horizontal fracture zones only	†	1·RM	1000·RM	
Extended zones	†	100·RM	1000·RM	1000·RM

† Either depth or non-depth dependent.
‡ Dependent on type of contrast chosen.

2.5 Finite element model

2.5.1 General

The finite element code NAMMU has been used to solve the groundwater flow equations. NAMMU is a deterministic porous media model used extensively in previous SKB projects. In conjunction with NAMMU, the HYPAC package has been used for pre- and postprocessing. The finite element models have been discretized with the same equidistance as the topography data obtained with the SKB GIS-system, that is roughly 50 meter elements in the horizontal direction. Vertically the elements are smaller at the surface, about 45 metres and larger at the bottom, 200 metres.

Vertical fracture zones have been modelled explicitly using specially designed elements for the fracture zones, whereas the subhorizontal fracture zones have been introduced using the implicit fracture zone method [*Kemakta, 1993*].

In the implicit method the elements intersected by fracture zones are assigned hydraulic conductivities that are weighted averages of the fracture zone conductivity and the rock-mass conductivity. In this way the mesh generation is greatly facilitated.

The implicit fracture zone method has hitherto only been implemented for three-dimensional models. Therefore, the mesh generated in the present study consist of one layer of eight-node brick elements.

2.5.2 Variations

I order to investigate the effect of the position of the upstream boundary, three different regions called R1, R2 and R3 were analyzed. As mentioned in Section 2.3.1 all three models end at a vertical fracture zone. Variations in model dimensions and data on finite element model sizes are shown in Table 2.4. The shorthand naming of the different variations is defined in Appendix A.

Table 2.4 Geometric variations and finite element model sizes.

Model	Xmin [m]	Xmax [m]	Zmin [m]	Zmax [m]	Elements	Nodes	Front width
R3S	0	42890	-3000	57	23850	49660	60
R2S	0	26146	-3000	40	14550	30316	60
R1S	0	17775	-3000	35	9875	20592	60

All in all the following variations have been studied (fracture zone patterns and contrasts are defined in Sections 2.4.2 and 2.4.3 respectively):

- Three homogeneous models with the three different model domains with depth dependent permeability.
- The three different model domains with fracture pattern 1, depth dependent permeability and high contrast between fracture zones and rock mass.
- The three different model domains with fracture pattern 2, depth dependent permeability and high contrast between fracture zones and rock mass.
- Small model domain with fracture pattern 3, depth dependency and high contrast.
- Small and medium model with fracture pattern 4, depth dependency and high contrast.
- Small and medium model with fracture pattern 5, depth dependency and high contrast.
- Small and medium model with only vertical fracture zones. Zone 2 (see SKB 91 [*SKB, 1992*]), depth dependency and high contrast.
- Medium model without vertical fracture zones, horizontal fracture pattern 1, depth dependency and high contrast.
- Small model with fracture pattern 1, depth dependency and small contrast.
- Small model with fracture pattern 1, no depth dependency and high contrast.

3 Results

3.1 General

The following chapter presents the results from the calculations performed. For a detailed description of the nomenclature used for the various cases refer to Appendix A. The results are presented in the following order:

- In Section 3.2 different methods for postprocessing that were used are summarised.
- Section 3.3 illustrates the effects of varying the model domain size, first for the homogeneous models and then for the models including fracture zones.
- In Section 3.4.1, the results from fracture patterns 1, 2 and 3 are compared.
- In Section 3.4.2, fracture patterns 4 and 5 with extended subhorizontal fracture zones are discussed.
- In Section 3.4 3, the results from variations with only one subhorizontal fracture zone (Zone 2 in SKB 91) are described.
- A comparison with some of the results obtained in SKB 91 is made in Section 3.5.
- Finally, Section 3.6 presents the results of some miscellaneous variations that were performed during the study.

3.2 Type of postprocessing

The results which are created by NAMMU [*Hartley and Jackson, 1992*] are the distribution of hydraulic head in the model. Different kinds of postprocessing must be performed in order to provide an understanding of the model results. The HYPAC program TRG [*Kemakta, 1993*] and different kinds of visualization tools have been utilized.

By using TRG the hydraulic head and permeability distribution have been surveyed for the different fracture patterns and positions of the upstream boundary. Head and permeability have been evaluated on a rectangular grid with 100 m times 50 m distance between the grid points. The main tool for the evaluation of flow around the repository area is the use of particle tracking which also has been performed with TRG.

The term particle tracking can be somewhat misleading. In the following sections, particle tracking refers to groundwater travel only, not taking dispersion or any solute-rock interaction mechanisms into account.

Pathlines have been started at positions along two lines, one vertical at x=16 000 m and one horizontal line at 600 m depth in the part of the domain that corresponds to the intersection with the HYDRASTAR block in SKB 91, see Figure 2.3. As mentioned in Sections 2.3.1, the part of the model domain that intersects the actual repository is only less than 10% of the intersection with the HYDRASTAR block. The line marked "Repository" in the figures refers to the starting position for the particle tracks.

The results have only been presented up to an x-coordinate of 20 000 m i.e., a position between the R1 and R2 boundaries. The reason for this is that the main objective of the project was to study the groundwater movements in the repository area and not further upstream. The results from the R1 model only span from 0 m to about 17 800 m since this is the actual horizontal extension of the R1 model. All models have a vertical extension from the ground surface to -3000 m depth, but some visualizations of the particle tracks are made of a smaller area to better illustrate the paths in the vicinity of the

repository. Since the particle tracks only show the geometry of the flowpaths and travel times, the stream function was calculated for the homogeneous case (R1SDN) and for the model with only one subhorizontal fracture zone (R1SDVV). Some particle tracks do not discharge at the model boundary. This is an effect of the algorithm used when performing the postprocessing. Particle tracks may end for two reasons other than reaching the model boundary. Either the gradient is considered to be too small to effectively carry on the particle tracking or the particle has visited the same model element too many times.

3.3 Results with a varying model domain

3.3.1 Effect of model domain on head distribution and flow pattern.

Simulations with a varying model domain have been performed for a set of conductivity distributions, first for the homogeneous case and then for fracture patterns 1 and 2. The largest model domain R3 gave no significant difference concerning head distribution and particle tracks compared to the R2 region in the area of interest. The presentation below is therefore focussed on comparing the results for the R1 and R2 domains.

Homogeneous models

For the comparison of the homogeneous cases with model domain R1 and R2, Figure 3.1 illustrates the differences in hydraulic head distribution. The difference is small and most visible in the vicinity of the upstream boundary to the left in the figure.

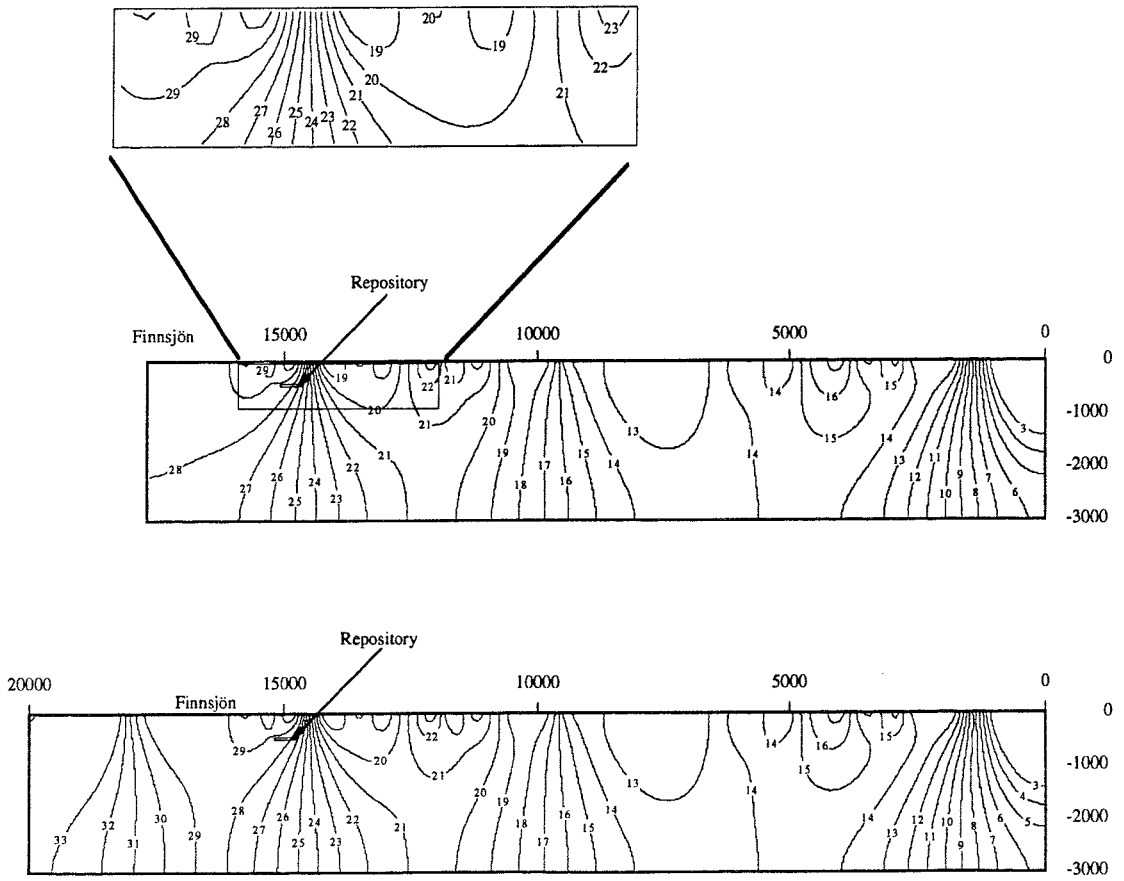

Figure 3.1 Head distribution for the R1 (top) domain and part of the R2 domain for the homogenous case with permeability decreasing with depth.

Particle tracks for the modeled sections R1 and R2 without any fracture zones are shown in Figure 3.2. There is a clearly visible difference between the particles that were released close to the R1 boundary. The effect of the boundary of model R1 on the flow pattern direct particles closer to the model bottom but the flowrate at those depths is very low. The influence on the particles released in the repository block is much smaller. The reason for this is both that they are released further from the R1 boundary and that the effect from the additional regional topography included in the R2 model is less pronounced closer to the surface. A comparison of the groundwater travel times of the particles released in the repository block is given in Section 3.3.2.

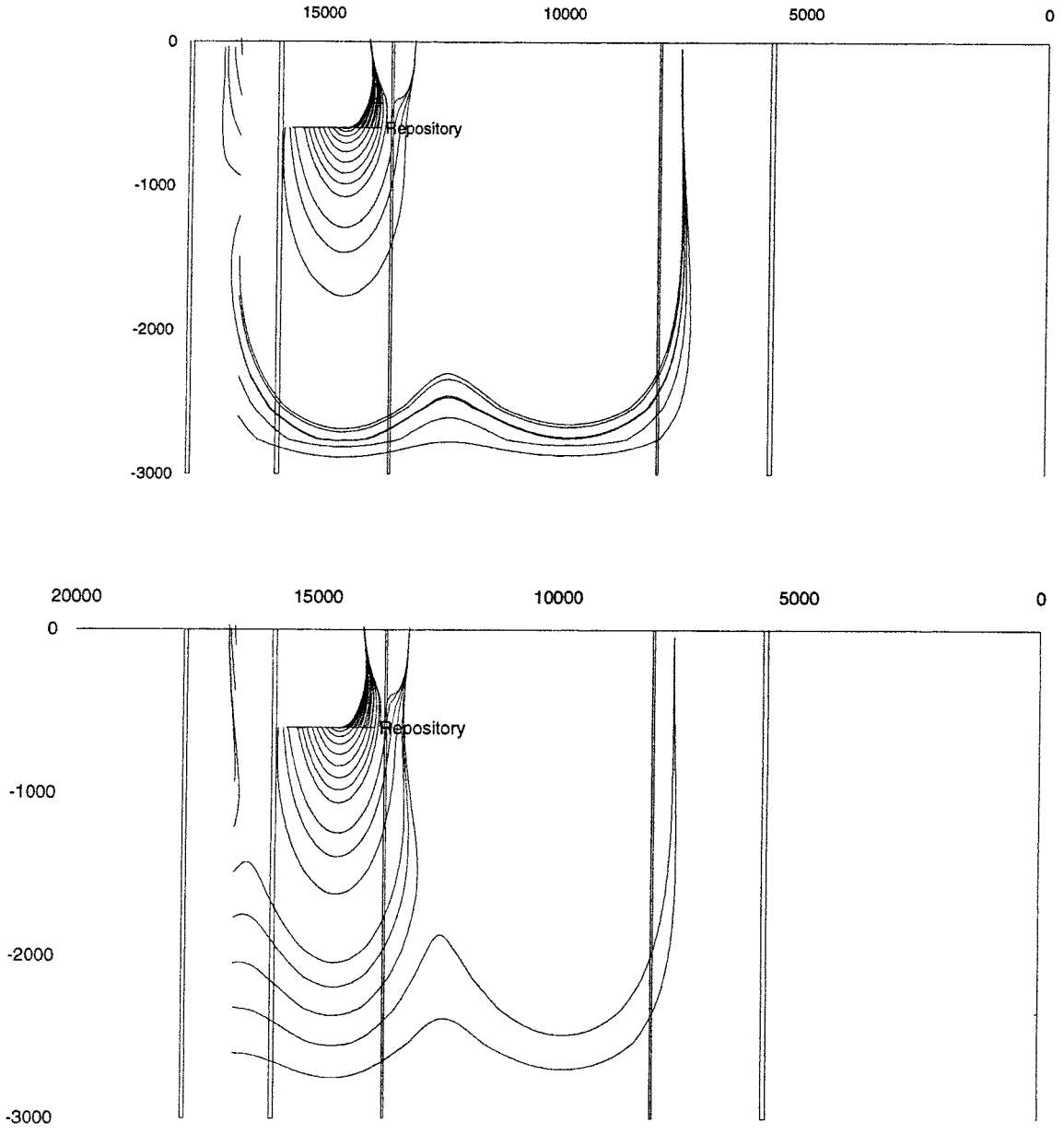

Figure 3.2 *Particle tracks for model section R1 (top) and R2 for the homogenous depth dependent permeability distribution. Note that the vertical fracture zones are only included in the figure to aid orientation, they were not included in these homogeneous cases.*

To get a better understanding of the flow situation in the part of the model that is closest to the surface, the stream function for the upper 1000 metres for model section R1 was calculated. The physical meaning of the stream function is that the amount of water passing a line between two points is given by the difference in the values of the stream

function at the two points. This means that in an equidistant contour plot of the stream function the same amount of water will pass between two consecutive contour lines. In Figure 3.3 a contouring of the stream function for model section R1 for the homogeneous case is shown.

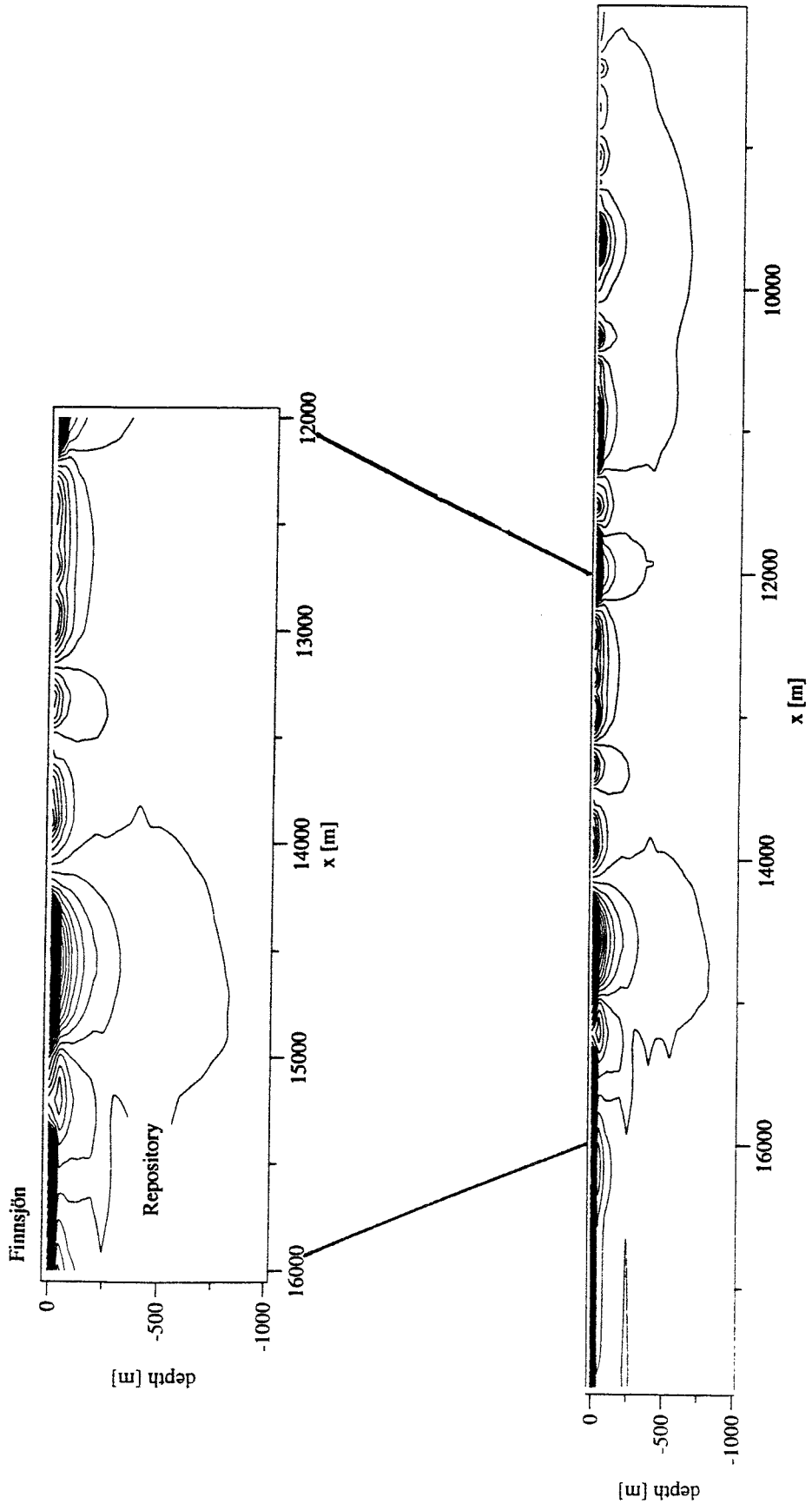

Figure 3.3 *Stream function for homogeneous model domain R1. The flow between two lines is 1.6 m³/year.*

Models with fracture zones

When comparing the particle tracks from the model with fracture pattern 1 with the three different model domains the results from model domains R2 and R3 were identical as for the homogeneous case. Differences occur between model domain R1 and R2 but mainly for the particles started along the vertical line on the left in the pictures. It is important to notice that the intersection of the A-A'-section with the repository is only a *small part* on the left side of the horizontal line along which particles have been started, see Section 3.2. There is no significant differences between the particles released in the repository block at 600 m depth for model domains R1 and R2 with fracture pattern 1 (Figure 3.4).

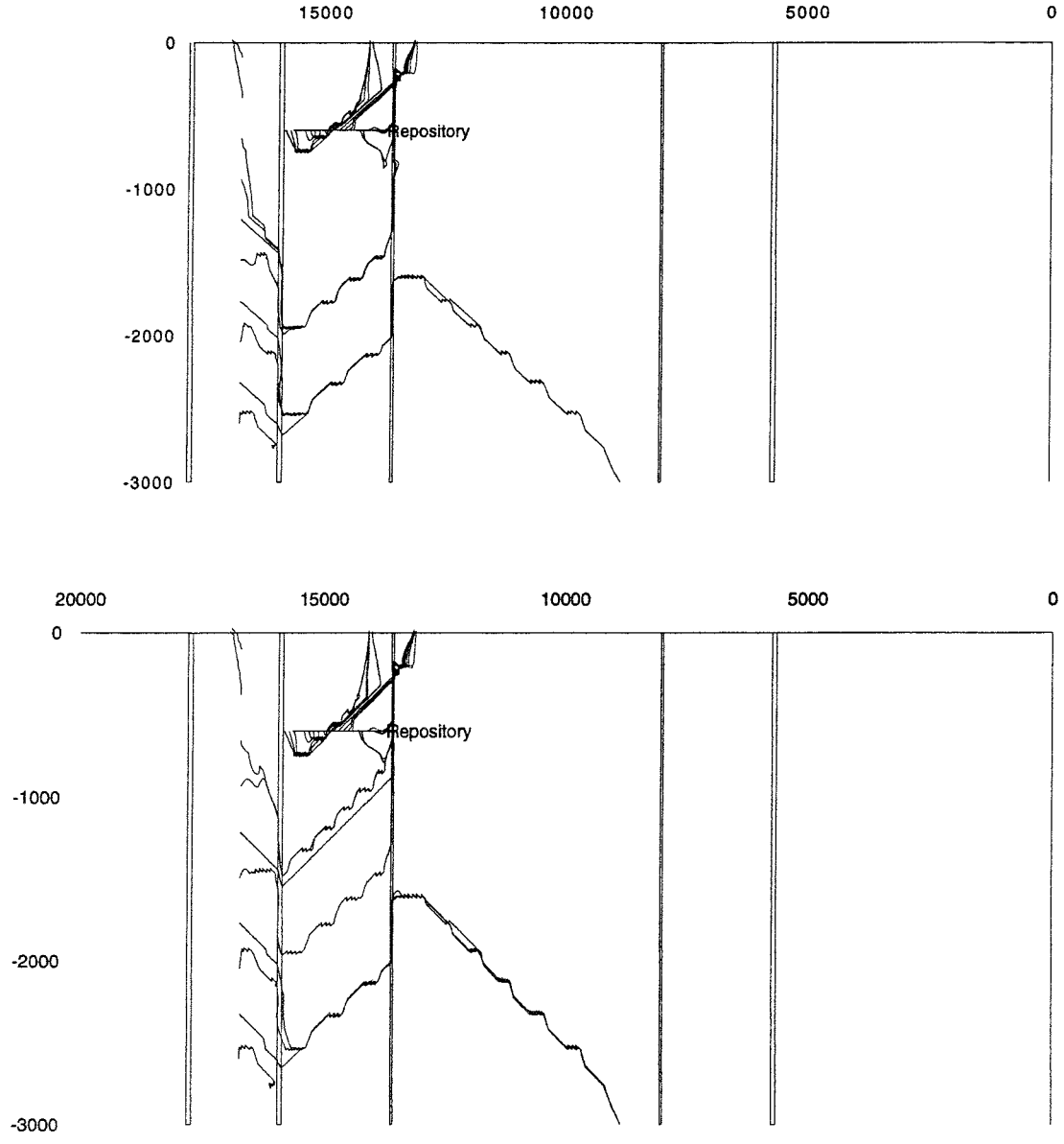

Figure 3.5 Particle tracks with model section R1(top) and R2 for fracture pattern 1.

With fracture pattern 2 (pattern without displacement of the horizontal fracture zones at the intersections with the vertical fracture zones) the difference between the particle tracks with model domain R1 and R2 are more obvious than with fracture pattern 1 and the homogeneous cases. As can be seen in Figure 3.5 all particles released in the repository block reach the surface at the same location for model domain R2 as compared to two locations with model domain R1. There in no general conclusion that can be drawn from this since such details of the flow pattern is dependent on the actual location of individual zones and the local gradient situation.

There is no significant difference between the particle track released along the vertical line, to the left in the figures, for fracture pattern 2.

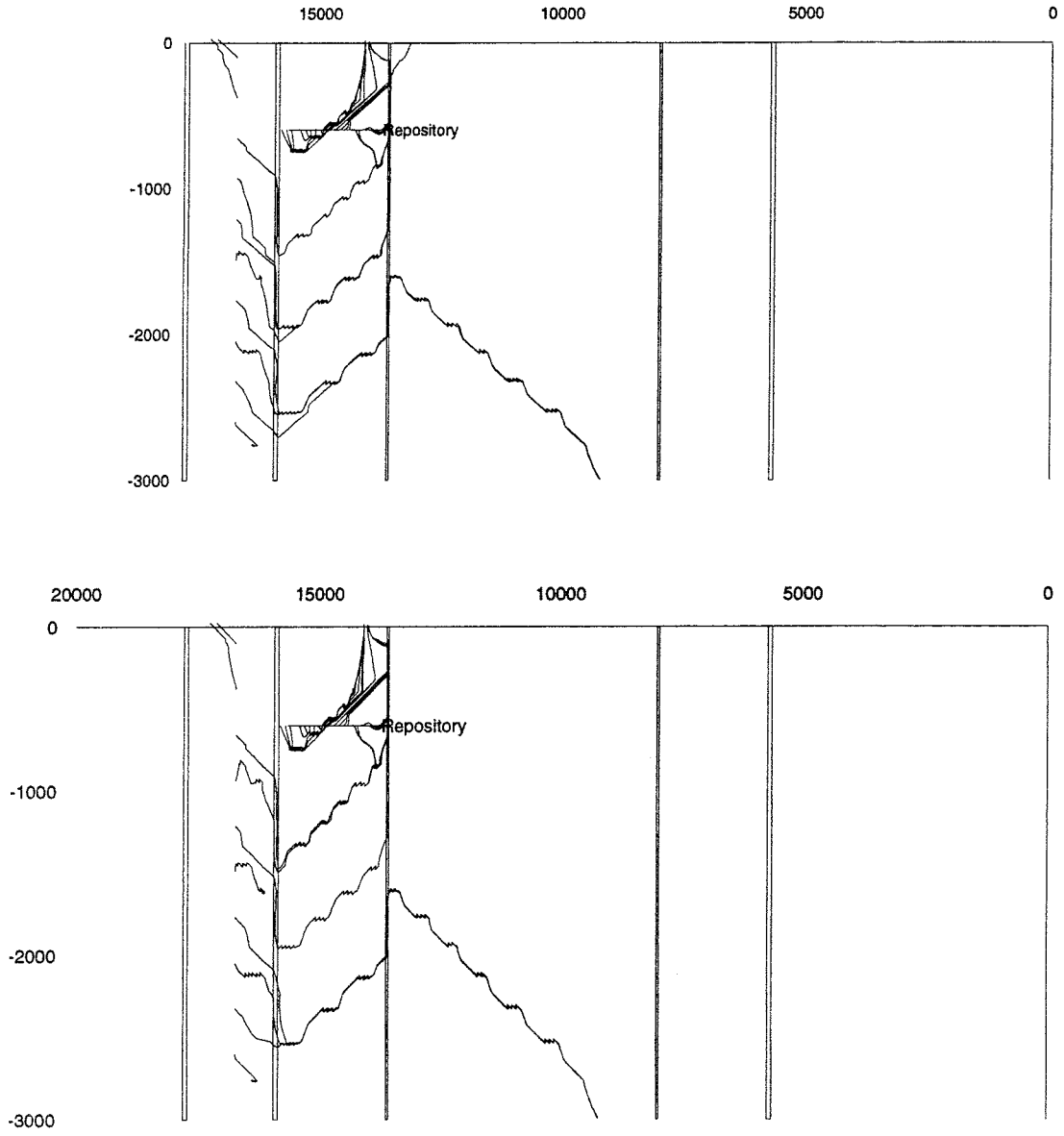

Figure 3.7 Particle tracks with model section R1(top) and R2 for fracture pattern 2.

A large part of the distance travelled by the particles is within the subhorizontal fracture zones. Almost all of the particles released in the repository block are transported within the same fracture zone irrespective of the boundary condition (R1 and R2) for both fracture patterns 1 and 2.

3.3.2 Effect of model domain size and fracture zone pattern on the groundwater travel time

Since it is hard to visually compare all aspects of the particle tracks, statistics on the groundwater travel times were calculated for the particles that were released in the repository block. The results are shown in Table 3.1 and Figure 3.6. Note that the scales on the axes are different in the figure. It is interesting to see in Table 3.1 that for the larger model domain (R2) the median travel time is virtually the same as for the small domain (R1) when the same fracture pattern is used. The difference in mean travel time is mainly due to decrease in travel time for particles with a very long residence time for model domain R2. The same tendency exists for most of the models with fracture zones as well as for the homogeneous models.

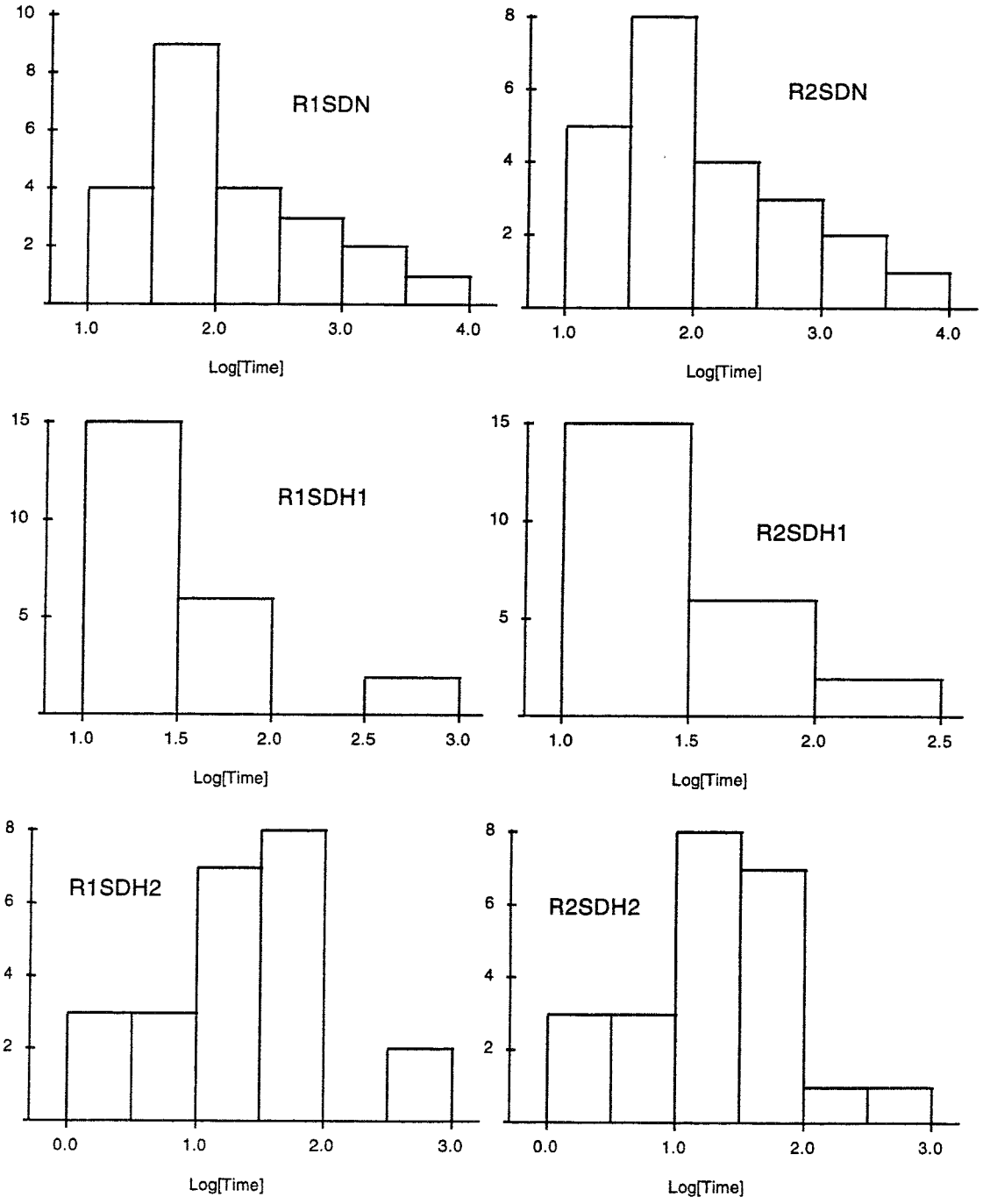

Figure 3.6 *Histogram of Log[Travel Time in years] for model section R1 (left) and R2. See Appendix A for explanation of the case names.*

Table 3.1 *Statistics on groundwater travel time for particles released in the repository block at 600 m depth. The number of particles is 23.*

Case	Mean [Years]	Median [Years]	Min [Years]	Max [Years]
R1SDN	496	80	27	4689
R2SDN	419	79	27	3507
R1SDH1	56	22	3.8	364
R2SDH1	46	20	3.7	288
R1SDH2	58	21	0.7	447
R2SDH2	49	20	1.2	325
R1SDH4*	313	9.3	1.7	1808
R2SDH4*	338	7.6	1.3	2183
R1SDH5*	15	11	2.4	63
R2SDH5*	15	11	2.9	56
R1SDVV*	146	73	26	590
R2SDVV*	142	72	27	587

*Not included in Figure 3.6.

As is obvious in Table 3.1 the differences in travel times between the two model domain sizes are small for all fracture patterns including the two cases with only Zone 2 and vertical zones. The particle tracks for fracture zone patterns with extended fracture zones (pattern 4 and 5) are shown in Section 3.4.2. The two models with only one horizontal fracture zone (R1SDVV and R2SDVV) are further discussed in Section 3.4.3.

3.4 Influence of the model fracture patterns

3.4.1 Effect of fracture pattern on head distribution and flow pattern

For the five different fracture patterns described in Chapter 2, the head distribution is presented as raster images since the influence of the heterogeneity of fracture zone structures on the head make line contour diagrams hard to interpret.

In Figure 3.7 the five head distributions for fracture patterns 1 to 5 with high permeability contrast between fracture zones and rock mass is shown. The corresponding log-permeability patterns are shown in Figure 2.7. The differences between the head distributions are minor. Fracture pattern 3 give a more homogeneous impression which was expected.

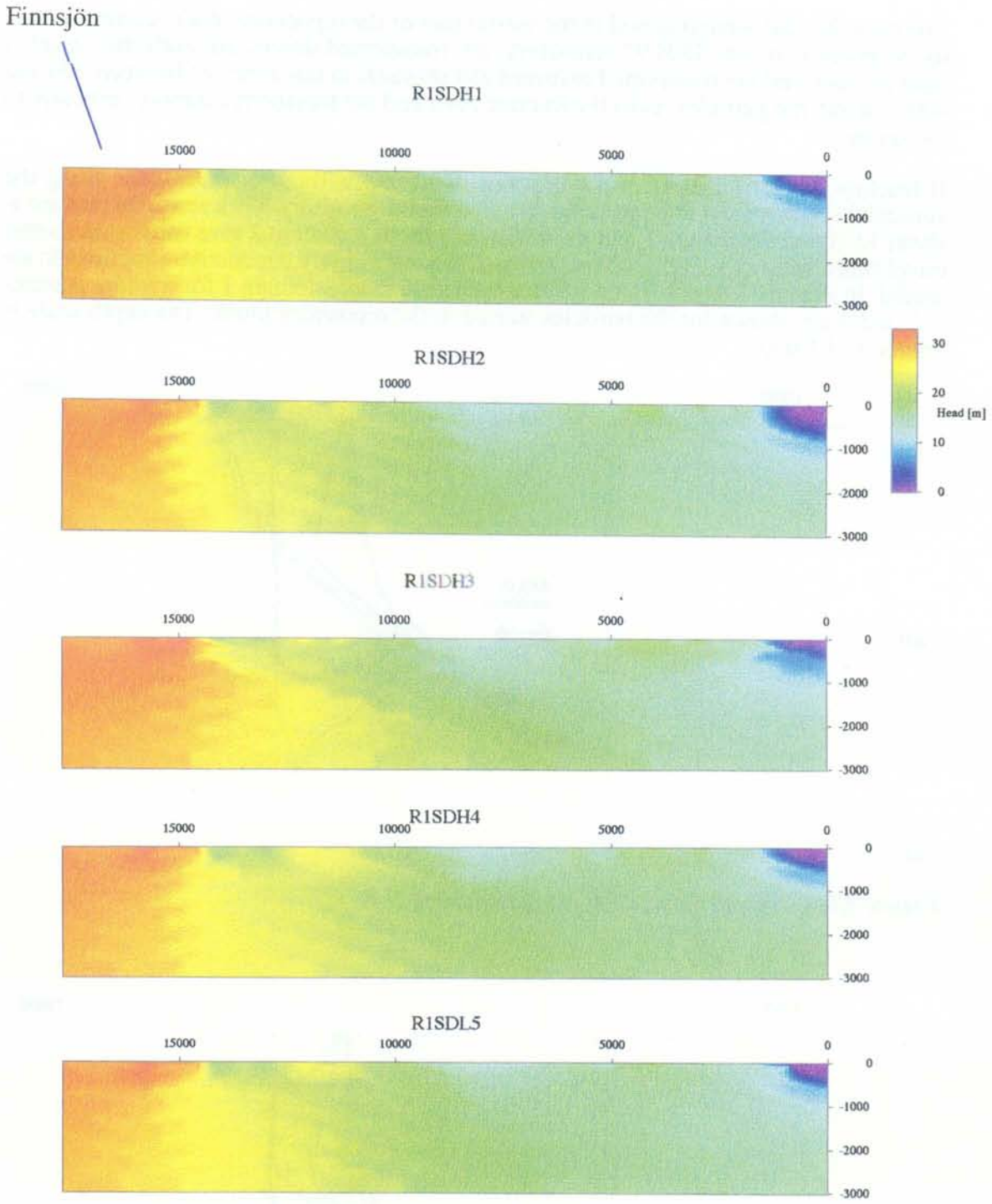

Figure 3.7 *Head distribution for the five fracture patterns with high permeability contrast between rock mass and fracture zones. The shown domain is R1 for all five patterns. Pattern 1 at the top and pattern 5 at the bottom.*

The particles that were released in the wester part of the repository block, corresponding to the position of the SKB 91 repository, are transported downward until they reach a fracture zone and are transported eastward and upwards in this zone. At between 300 and 400 m depth the particles leave the fracture zone and are transported almost vertically to the surface.

If fracture patterns 1 and 2 are compared (with and without displacement along the vertical fracture zones) most particles released in the repository block reach the surface at about 13 100 m for pattern 1 and at 14 050 for pattern 2. Pattern 2 give somewhat shorter travel times due to the higher connectivity of the most highly conductive structures in the model. In Figures 3.8 to 3.10 the particle tracks for model domain 1 for fracture patterns 1, 2 and 3 are shown for the particles started in the repository block. The depth scale is limited to 1000 m.

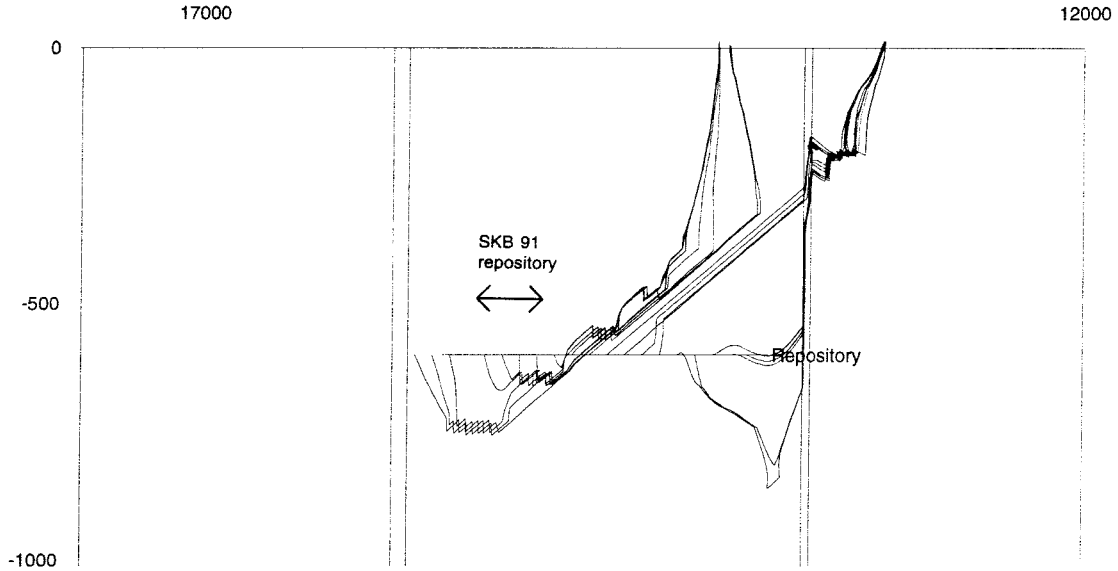

Figure 3.8 Model domain R1, fracture pattern 1.

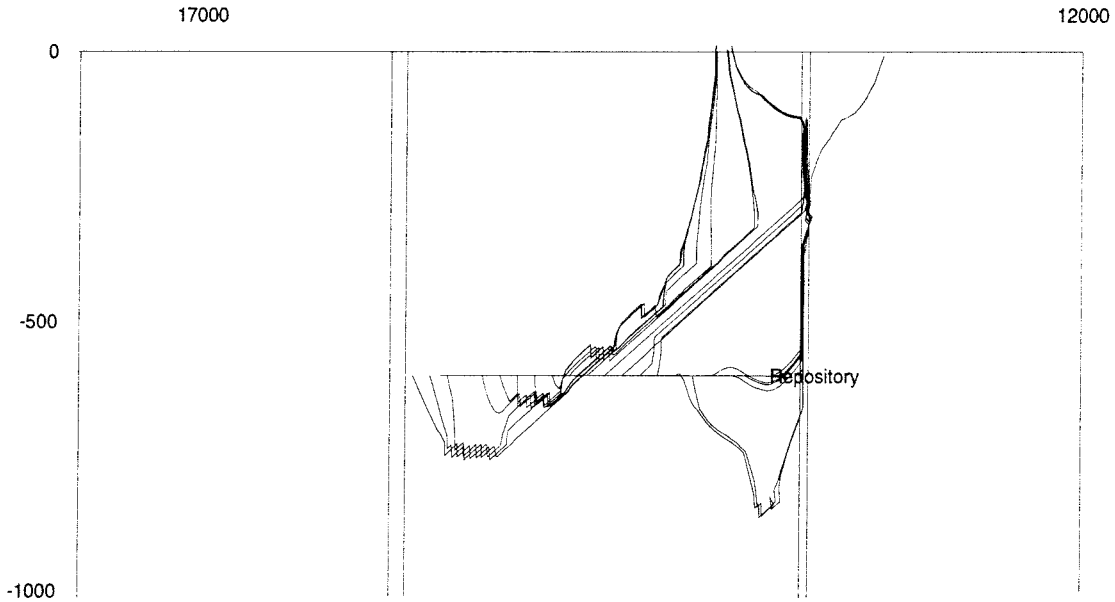

Figure 3.9 Model domain R1, fracture pattern 2.

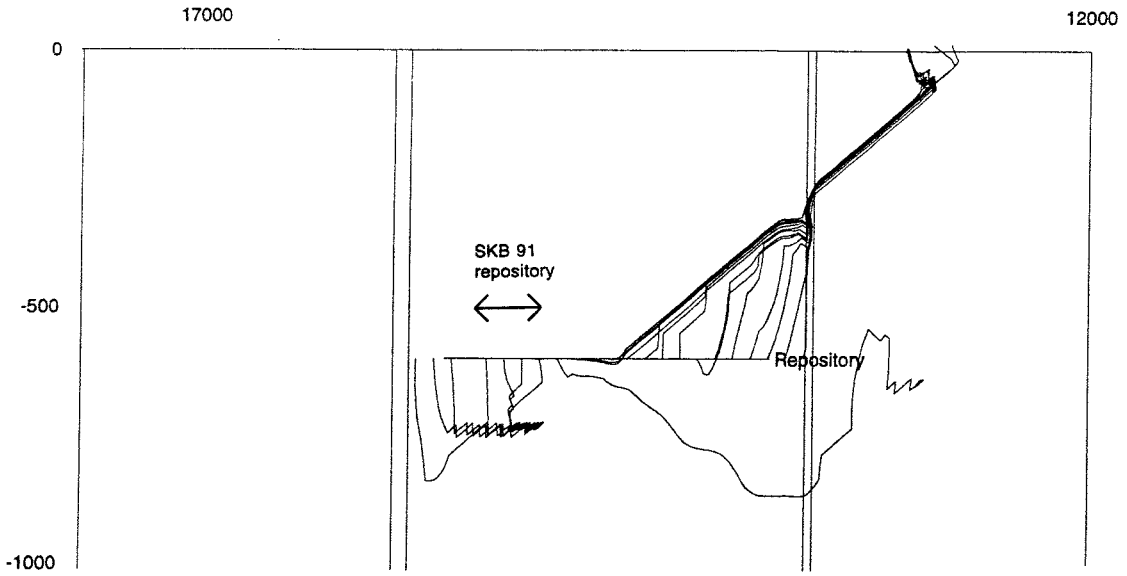

Figure 3.10 Model domain R1, fracture pattern 3.

With fracture pattern 3 (Figure 3.10) the particles released in the left part of the repository block are first transported downwards as in all other cases. At about 700 m depth these particles reach a model section with such a small pressure gradient that the particle tracking algorithm is aborted. The particles that were released in the right part of the repository block are transported to a subhorizontal zone and migrate within this fracture zone to the surface.

3.4.2 Models with extended fracture zones

As have been shown earlier, fracture patterns 4 and 5 include an extended subhorizontal fracture zone that intersects a major part of the models, see Section 2.4.2 and Figure 2.7.

Fracture pattern 4 is different from the others regarding the distance travelled by particles released in the repository block. As is shown in Figure 3.11 some particles reach the long horizontal fracture zone passing below the repository. With fracture pattern 4 and model domains R1 and R2 particles actually reach all the way to the Baltic Sea, see Figure 3.13. Although a part of the particles in fracture pattern 4 have very long groundwater travel times, this patterns result in short median travel time when all particles starting in the repository block are considered, see Table 3.1.

The effect of the extended zone in fracture pattern 5 (see Figure 3.12) is significantly less pronounced than for fracture pattern 4. The head distribution with fracture pattern 5 did not result in any particles released in the repository block reaching the extended fracture zone. The results where the same of both model domain R1 and R2 using fracture pattern 5. The particle tracks using model domain R2 and pattern 5 is included in Appendix C.

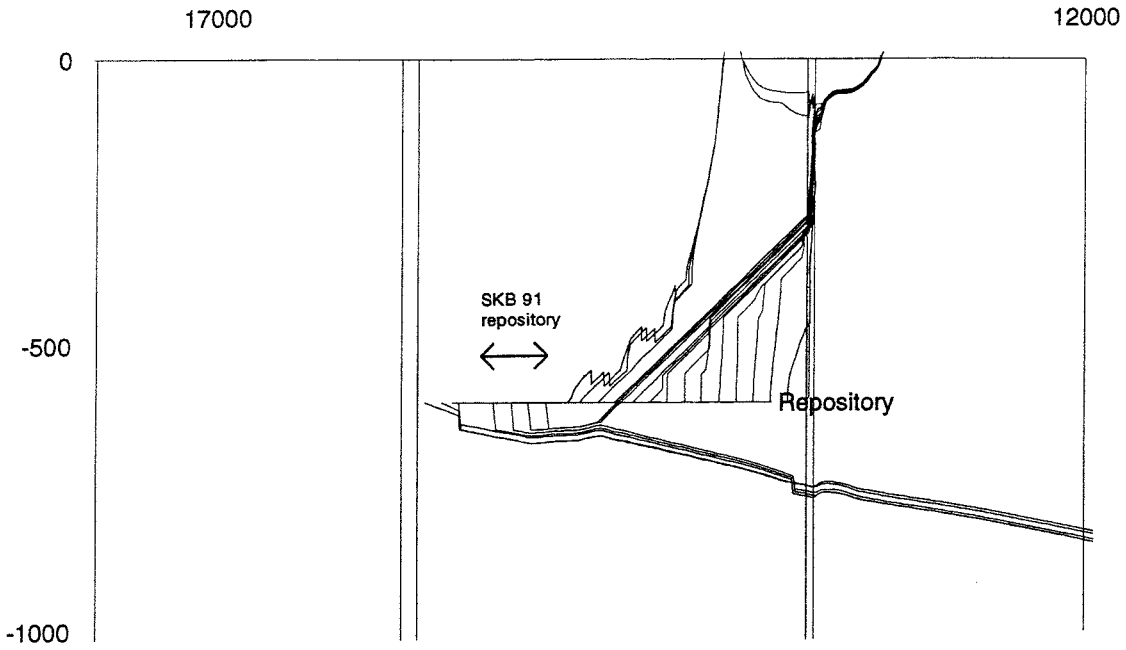

Figure 3.11 Model domain R1, fracture pattern 4.

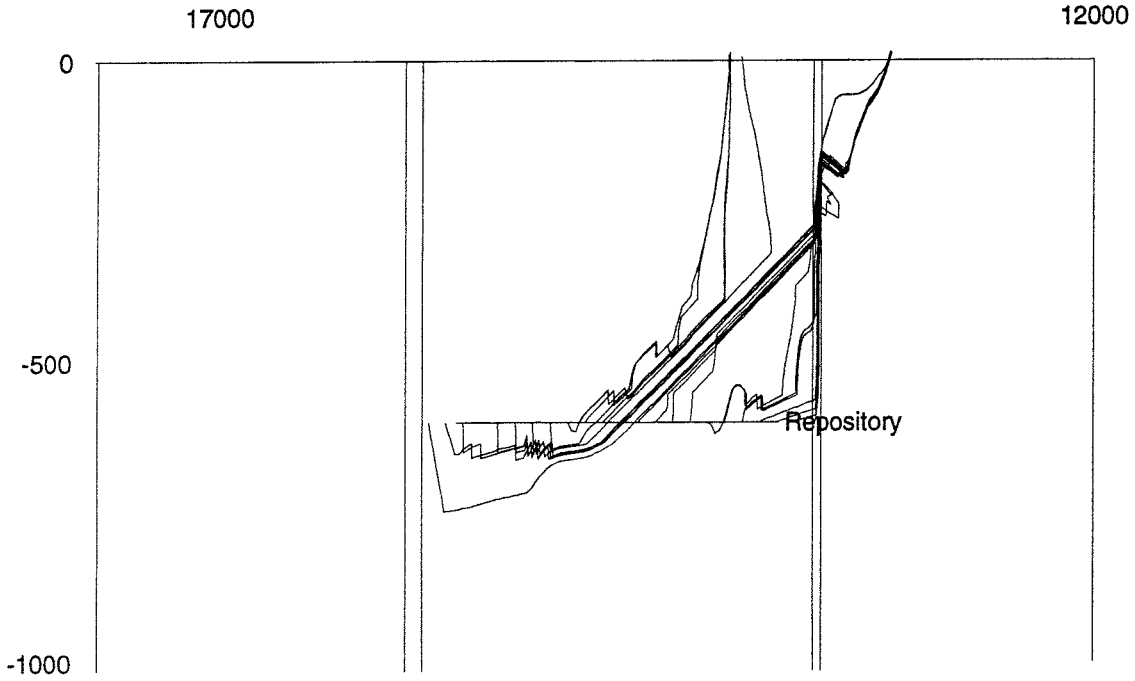

Figure 3.12 Model domain R1, fracture pattern 5. Compare with Figure 3.8.

In cases R1SDH4 and R2SDH4 (Figure 3.13) all particles released in the left part of the repository block, where the repository was located in SKB 91, reach the extended sub-horizontal fracture zone and result in long travel times.

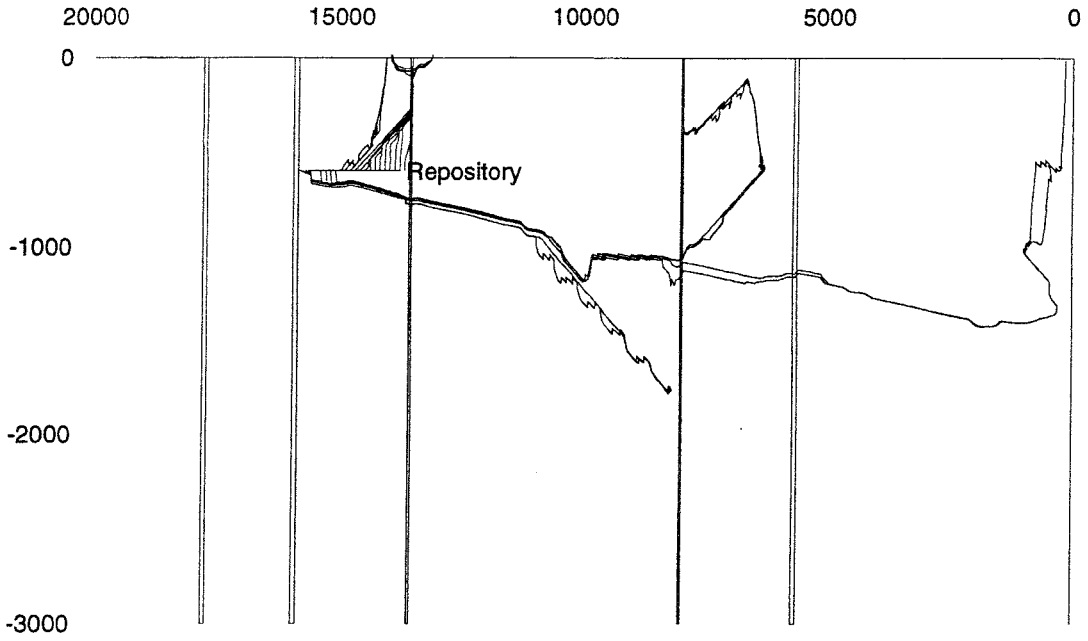

Figure 3.13 Model domain R2, fracture pattern 4.

3.4.3 Models with a single subhorizontal fracture zone

To produce a model that was to some extent comparable to the SKB 91 model, one fracture pattern without the horizontal fracture zones (Zone 2 from SKB 91 was still included) was constructed. The results of these two variations, R1SDVV and R2SDVV, without the horizontal fracture zones are similar to the homogeneous model except that all particles released into the repository block reach the surface at the same location. The reason that all particles in Figure 3.14 reach the surface to the left of the fracture zone is that the Imundbo zone intersects the surface of the model at a higher altitude than the section at x=14 000 m. This is illustrated in Figure 3.15 where the elevation and other important features around the repository block are shown. Particle tracks for model R1SDVV are shown in Appendix C.

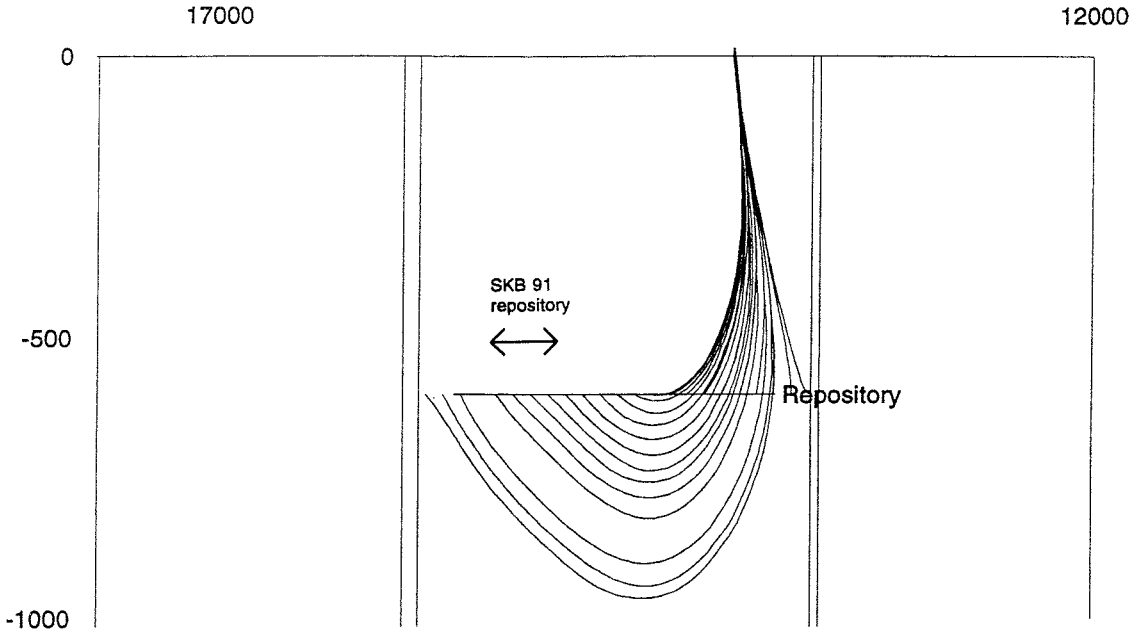

Figure 3.14 *Model domain 2 without horizontal fracture zones, Zone 2 from SKB 91 is included. Case R2SDVV. Compare with Figure 3.3.*

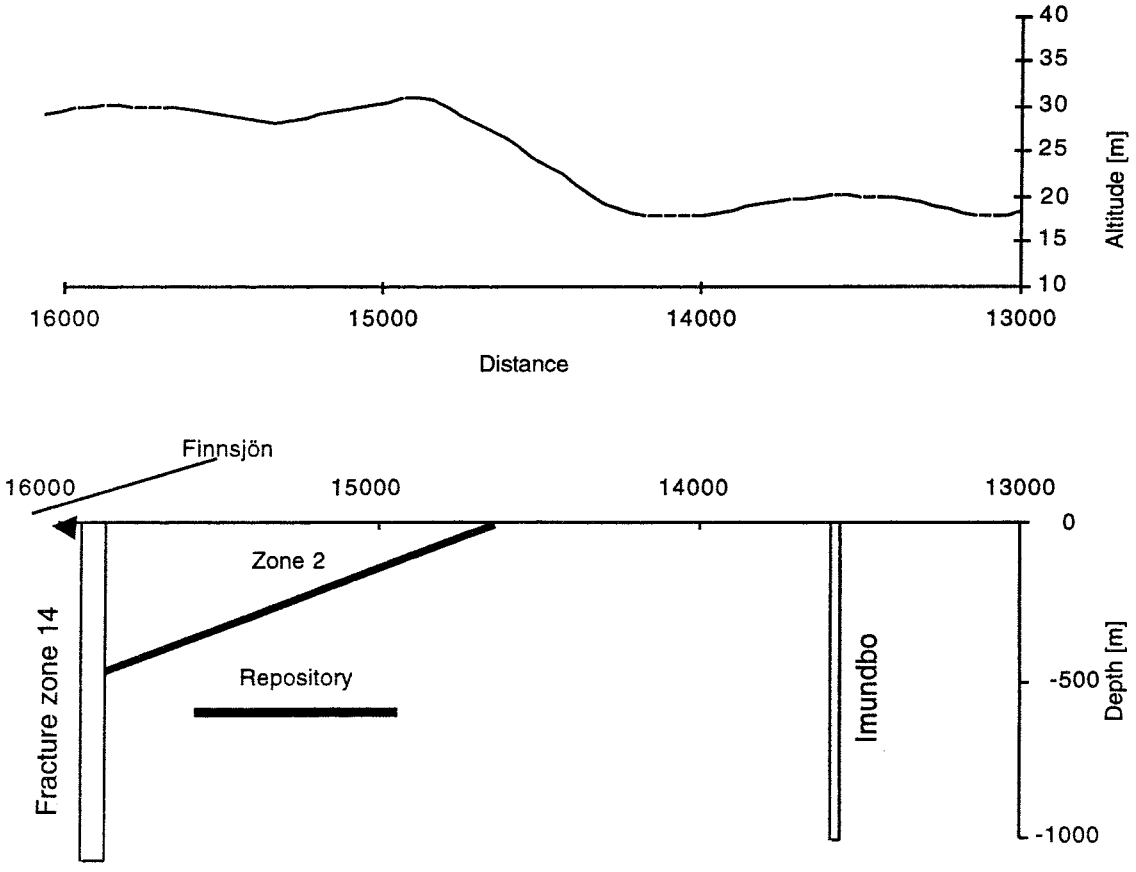

Figure 3.15 *Topography and position of important features around the repository block.*

To study the water flow in more detail, the stream function was calculated for case R1SDVV, see Figure 3.16, in the same way as for case R1SDN in Figure 3.3. Fracture zone 2 is obviously the dominating water-conducting feature in this model. It is important to recognize that the contour interval in Figure 3.16 is such that the water flow between to adjacent streamlines is 16 m^3/year, i.e., 10 times higher than for the stream function in Figure 3.3.

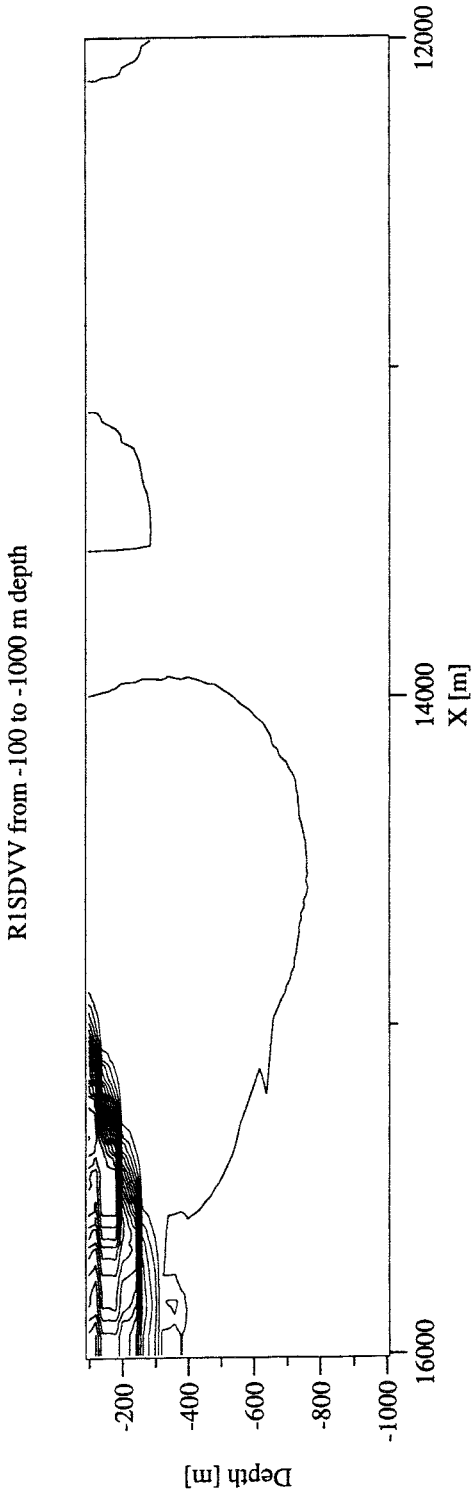

Figure 3.16 Stream function for case R1SDVV. Compare with Figure 3.3.

3.5 Comparison with results from SKB 91

Within SKB 91 a three-dimensional finite element model was created to form a reference case for the far field flow analysis. This reference case, reported in [*Lindbom and Boghammar, 1992*], was named X36. The outline of that model is shown in Figure 2.3.

Generally it is difficult to compare results from a two-dimensional model with those obtained with a three-dimensional model. The differences between the models created for this project and the X36 case from SKB 91 are apart from dimensionality:

- The vertical extension of the X36 model was only 1500 metres while the depth of the model is 3000 m in the present study.
- There are some additional vertical zones included in the X36 model crossing the A–A'-section (Zones 1 and 4, Giboda and Giboda S, NS1 and NS2). These zones were interpreted on a local scale and are therefore not included in the present study.
- As can be seen from Figure 3.17 the topography along the A–A'-section had a smoother appearance in the X36 model than in this study.
- All fracture zones in the X36 model were modelled using the implicit fracture zone method.

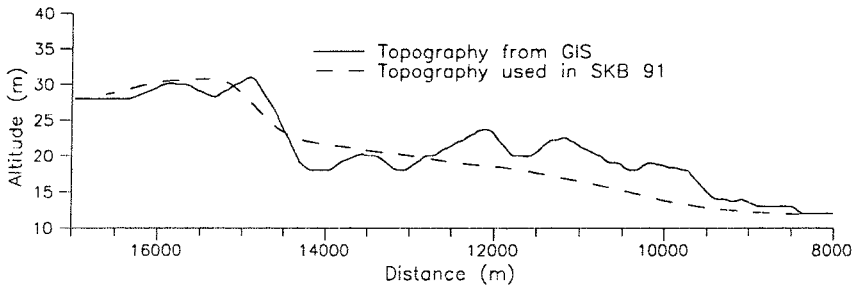

Figure 3.17 Topography along the A-A'-section used in SKB 91 and GIS-generated topography used in the present study.

Apart from these differences the models have the same hydraulic conductivity depth dependency assigned to the rock mass and approximately the same location of the upstream lateral boundary, that is the R1 model domain in this study. All zones included in the present study that lie within the SKB 91 model domain were also included in the X36 model, apart from the generic sub-horizontal zones introduced.

The closest comparison would be to compare the X36 case with R1SDVV and R2SDVV, the cases with model domain R1 and R2 and only vertical fracture zones except for the sub-horizontal Zone 2. In addition the R1SDN case (model domain R1 with homogenous rock) could be used for comparison.

The pressure field obtained with the X36 model along a vertical cross-section roughly aligned with the A–A'-section shows a fairly smooth horizontal pressure drop from the inland towards the Baltic sea. This is of course due to the smooth topography used within the SKB 91 study, see Figure 3.17. The model calculations performed within the present study show the same general pattern but with several local discharge areas induced by the more detailed topography.

In SKB 91 the major discharge of groundwater passing through the repository was along the topographical gradient aligned roughly with the A–A'-section to the vertical zone Imundbo (vertical fracture zone 3 in this study), and along the Imundbo zone to the model boundary. The groundwater travel path was directed downwards at the repository. The mean value of the accumulated travel times from the repository was $4.5 \cdot 10^2$ years. It is fair to assume that the major time was spent in the rock mass and that the passage through the Imundbo zone was comparably rapid.

All models in the present study show the same general groundwater pathways for groundwater passing through the repository, i.e. first downward and then eastward and upward. In the cases including the generic fracture zone patterns a sub-horizontal zone located close below the repository acts as a collector for the pathways. For case R2SDVV the mean travel time from the repository was $1.4 \cdot 10^2$ years and for case R1SDVV $1.5 \cdot 10^2$ years. For the homogeneous case R1SDN the mean travel time was $6.7 \cdot 10^2$ years i.e. the homogeneous case and cases R1SDVV and R2SDVV gave mean travel times that were comparable with the $4.5 \cdot 10^2$ years obtained in SKB 91.

The small difference in groundwater travel times between the two different positions of the boundary for the 2-D model is an indication, but not an evidence, that the effect of using a larger 3-D model in SKB-91 would have been minor at repository depth.

There are obvious similarities between the flow patterns calculated in the present study and those obtained in SKB 91 [*Lindbom and Boghammar, 1992*]. It should be noted that the average permeability in the domain varies significantly between the different cases due to the variable amount of fracture zones that have been included. This means that care should be taken when drawing conclusions from comparisons between dissimilar cases.

3.6 Results from miscellaneous variations

One model without any depth-dependence on the permeability and finally one case with low contrast between fracture zones and rock mass (10 times) were modelled.

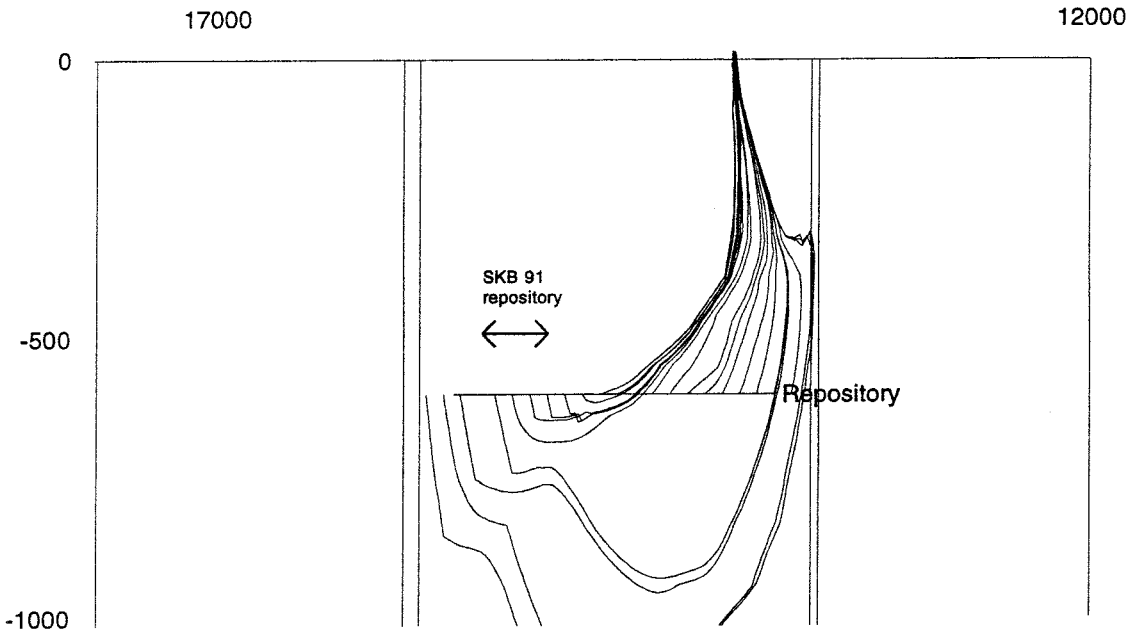

Figure 3.18 *Model domain 1, fracture pattern 1 with small contrast between fracture zones and rock mass. Case R1SDS1. Compare with Figures 3.8 and 3.2.*

The results with a smaller contrast between the fracture zone and rock mass gave particle tracks similar to those obtained with the homogeneous model. Some paths reach depths larger than 1000 m. All particles released in the repository block reach the surface at the same location as opposed to two different locations for the homogeneous model.

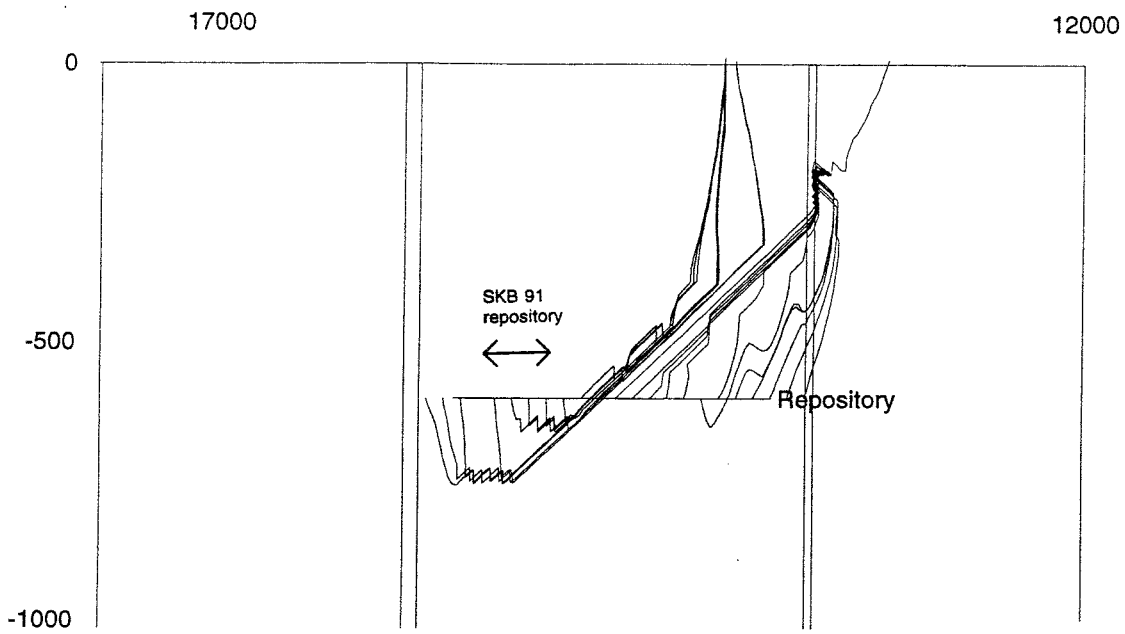

Figure 3.19 *Model domain 2, fracture pattern 1 without vertical fracture zones. Case R2SDR1. Compare with Figure 3.8.*

There is strong similarity between the results shown in Figure 3.19 and case R1SDH1 in Figure 3.8. Neither the depth dependence nor the exclusion of the vertical fracture zones changed the flow pattern to a large degree.

As expected, the case without depth dependence of the hydraulic conductivity gave no significant differences in comparison with case R1SDH1 in Figure 3.8. The particle track diagram for this variation is available in Appendix C.

4 Conclusions

To show the effect of varying the position of the upstream boundary, three different model regions named R1, R2 and R3 were studied. The R1 model is the smallest and have an upstream boundary that is approximately at the same position as the boundary that was used in SKB 91. The R2 and R3 boundaries are positioned further upstream at the intersections with large, regional, fracture zones.

None of the results from this study suggest that the model domain that was used for the NAMMU model in SKB 91 caused non-conservative results. Among all the evaluated fracture zone geometries and model sizes which have been evaluated there is none that stands out as a specially disadvantageous scenario, for example with flow directed upwards through the repository, that would significantly change the conclusions made regarding the groundwater pathways in SKB 91.

Concerning the choice of upstream boundary location, an improperly placed boundary will have the largest effect on the regional groundwater flow if there is a long almost horizontal conductive structure dipping in the direction of the regional gradient. The pressure in such an extended feature is mainly governed by the boundary pressure it will receive.

Generally a badly chosen location of a no-flow upstream boundary gives some marginally longer transport times for particles released in the vicinity of the repository. This is due to the fact that the water is forced to take a deeper route.

In the case with different generic fracture zone geometries the obvious conclusion have been that the higher the connectivity in the model the shorter are the travel times.

It has been noted during the course of this study that an early 2-D modelling can give valuable guidance regarding the potential importance of different features to be investigated in the site investigations. It is therefore suggested that a such a procedure is included in the site investigation programme. The experience regarding the coupling of topography generated by GIS and 2-D groundwater modelling suggest that the following stages are included as part of such a procedure in future projects:

- Generation of topography from the GIS-database along two or more parallel lines cutting through the potential repository region.
- Homogeneous two-dimensional models with the topography from GIS are modelled first (possibly with density variations due to salt content if salt is present at the site) including a sensitivity analysis.
- The topography and known fracture zones are used to generate two-dimensional models and generic fracture zone patterns can also be included at this stage.
- Potential repository sites are identified and the effect of the locations of model boundaries at these sites is studied to get information on suitable model size for the three-dimensional model.
- Perform 3-D modelling.

5 Acknowledgement

Comments from Roger Thunvik of the Royal Institute of Technology and Anders Ström of SKB that have significantly contributed to increase the quality of the report are greatfully acknowledged. Kaj Ahlbom of Conterra, who has written Appendix B of this report, has given a significant contribution to the geological basis for this study.

References

Ahlbom K, Andersson P, Ekman L, Tirén S (1987): Characterization of fracture zones in the Brändan area Finnsjö study site, central Sweden, SKB AR 88-09, Swedish Nuclear Fuel and Waste Management Company, June 1987.

Boghammar A (1993): Utredning av möjligheten att använda information från SKB's GIS-system vid generering av finita element modeller., Kemakta Konsult AB, SKB AR 93-10, Swedish Nuclear Fuel and Waste Management Company, Februari 1993 (in swedish).

Hartley LJ, Jackson CP (1992): NAMMU User Guide. Release 6.1, AEA Decommissioning & Radwaste, June 1992.

Kemakta (1993): Hypac User's Guide., Kemakta Konsult AB, Stockholm, March 1993.

Lindbom B, Boghammar A: (1992): Numerical groundwater flow calculations at the Finnsjön study site - extended regional area. SKB TR 92-03, Swedish Nuclear Fuel and Waste Management Company, March 1992.

Odin M: (1993): Personal communication.

SKB (1993): Users guide to HYDRASTAR 1.2, SKB AR 93-02, Swedish Nuclear Fuel and Waste Management Company, 1993.

SKB (1992): SKB 91; Final disposal of spent nuclear fuel. Importance of the bedrock for safety. SKB TR 92-20, Swedish Nuclear Fuel and Waste Management Company, May 1992.

SKB (1987): Slutlig säkerhetsrapport för SFR 1, Swedish Nuclear Fuel and Waste Management Company, 1987 (in swedish).

SKI (1992): Granskning av SKB 91, SKI TR 92:24, Swedish Nuclear Power Inspectorate, December 1992 (in swedish).

Voss C, Andersson J (1991): Some aspects of regional flow of variable-density groundwater in crystalline basement rock of Sweden., SKI TR 91:9, Swedish Nuclear Power Inspectorate, December 1991.

Appendix A

Modelling terminology and variations studied.

This appendix outline the model parameters that has been varied and the combinations that have been run.

Parameter definition :

The table below shows the definition of the parameters that has been varied.

Table A:1 Parameter definition.

Par.	Values	Description
xxx	R1S, R2S, R3S	Location of upstream lateral boundary
d	N(o),D(yes)	Depth dependence in rock mass permeability
c	N(o),H(igh),L(arge),S(mall), V(ertOnly),R(HorOnly)	Permeability contrast
p	N(o),1(displace),2(equal), 3(crossing), 4(extendedright), 5(extendedleft)	Subhorizontal fracture pattern.

The different variations performed have been named using the values listed in the table above in the parameter order "xxxdcp".

Cases studied :

Table A:2 Description and naming conventions for the performed variations.

No.	Variation	Description
1	R1SDN	Homogenous small model
2	R2SDN	Homogenous medium model
3	R3SDN	Homogenous large model
4	R1SDH1	Small model with fracture pattern 1, depth dependency and high contrast.
5	R2SDH1	Medium model with fracture pattern 1, depth dependency and high contrast.
6	R3SDH1	Large model with fracture pattern 1, depth dependency and high contrast.
7	R1SDH2	Small model with fracture pattern 2, depth dependency and high contrast.
8	R2SDH2	Medium model with fracture pattern 2, depth dependency and high contrast.
9	R3SDH2	Large model with fracture pattern 2, depth dependency and high contrast.
10	R1SDH3	Small model with fracture pattern 3, depth dependency and high contrast.
11	R1SDH4	Small model with fracture pattern 4, depth dependency and high contrast.
12	R1SDH5	Small model with fracture pattern 5, depth dependency and high contrast.
13	R1SDS1	Small model with fracture pattern 1, depth dependency and small contrast.
14	R1SNH1	Small model with fracture pattern 1, no depth dependency and high contrast.
15	R2SDH4	Medium model with fracture pattern 4, depth dependency and high contrast.
16	R2SDH5	Medium model with fracture pattern 5, depth dependency and high contrast.
17	R2SDVV	Medium model with vertical fracture zones only, including zone 2, depth dependency and high contrast.
18	R2SDR1	Medium model without vertical fracture zones, horizontal fracture pattern 1, depth dependency and high contrast.
19	R1SDVV	Small model with vertical fracture zones only, including zone 2, depth dependency and high contrast.

Appendix B

Gently dipping fracture zones in the Finnsjön region

Kaj Ahlbom

REVIEW

During the last years several attempts have been made to estimate the occurrence of gently dipping fracture zones in the Finnsjön region and in other parts of Sweden. These attempts have been summarized in SKB 91 and in the SKB progress report "Typberg in Finnsjönområdet" (Bedrock characteristics of the Finnsjön site, Ahlbom, 1991). Somewhat modified extract of these reports are presented below.

SKB 91

"To get some idea of how much general validity these data and interpretations have for the region, it is interesting to compare with the conditions in SFR and, to some extent, with the Dannemora iron mine. These two underground facilities lie within the same tectonic region as the Finnsjön area and can therefore, at least in part, be assumed to have been affected by similar tectonic forces.

What is particularly striking is the presence of major flat-lying fracture zones in all three areas. The frequency of these fracture zones at greater depth is unknown, but for the time being there is no reason to assume that they should occur at an appreciably different frequency that steeply dipping zones. Under the SFR facility, at a depth of 100-160 m below sea level, there is a highly permeable subhorizontal fracture zone. The width of this zone varies between 5 and 20 m. In the Dannemora Mine, rock blocks above subhorizontal faults are normally displaced towards the south in relation to the lower block". (SKB 91, pages 44-45).

Bedrock characteristics of the Finnsjön site

"The earlier sections have discussed steeply dipping fracture zones of different orders. It is reasonable to assume that there also exist corresponding horizontal or gently dipping zones. These zones could not be detected by geological mapping or by geophysical surveys performed at the study sites. Until recently, the only available data source has been borehole observations. Since the boreholes drilled at the SKB sites are 700 m or shorter the observation window is very limited. This in turn implies that only fracture zones with a spacing similar to the observation window or shorter can be expected to occur in the boreholes.

Table 1 presents a compilation of interpreted horizontal or gently dipping (0-30°) fracture zones at the SKB study sites. It is surprising is that at least three of the listed fracture zones have widths of 70 m or more. Using the ratio between extension and width commonly found for steeply dipping zones, these wide zones should be considered to have a regional extension. This in turn might have a large impact on regional groundwater flow, age of groundwater and groundwater chemistry. Possibly also on the bedrock stability. Judging from their widths only, other listed zones should be regarded as local fracture zones.

At least one gently dipping fracture zone have generally been interpreted within the c. 700 m long observation window. Roughly, this implies a corresponding spacing of these zones. An observation that calls for even shorter spacing is the possible existence of additional, unidentified, gently dipping zones. This is because the surface and borehole investigations made at the study sites were focused on steeply dipping zones, why a gently dipping zone, occurring only in boreholes, might have been misinterpreted as a steeply dipping zone or as fractured borehole sections not associated with any fracture zone.

Table B:1 *Occurrence of gently dipping fracture zones (0-30°) in the SKB study sites (mainly from Carlsson, Carlsson and Tirén, 1989).*

Site	No.of gently dipping zones	Width of zones (m)	Spacing (m)	Hydraulic contrast	Observation window (m)
Kamlunge	1	5-15	>550	-10^3	700
Gideå	1	10-25	>750	-10^3	700
Svartboberget	3	2-40	200-250	$>-10^2$	800
Finnsjön	1*	100	>500	-10^4	700
Fjällveden	-	-	-	-	700
Kråkemåla	1*	?	200-300	-10^3	600
CLAB	-	-	-	-	100
Ävrö	1	150	>400	-10^5	700
Klipperås	1	70	>750	-10^5	950
Sternö	-	-	-	-	800
SFR	1	3-16	>150	-10^2	250

* 1 "certain" fracture zone, possibly 2 additional zones

The occurrence of gently dipping zones have also been discussed with mining geologists from Kirunagruvan, Zinkgruvan and from the Boliden Company. The conclusion from these discussions is that, generally speaking, gently dipping zones occur in all mines and that, when comparing with steeply dipping zones, no major difference in occurrence nor properties could be identified. In some mines, however, steeply dipping zones are more common.

The Dannemora mine is an example of a mine with a frequent occurrence of subhorizontal to gently dipping fracture zones (Lager, 1986). These zones occur with a spacing of 300 m to more than 500 m. Where fault displacements have been observed, the rock block above a gently dipping fracture zone have always been displaced towards the south in relation to the rock block below the zone. The largest observed displacement on a gently dipping fault at Dannemora is 400 m.

In conclusion, gently dipping fracture zones have been identified in most of the SKB study sites. Probably, both 1st and 2nd order gently dipping fracture zones are represented but data are lacking for classification. A rough estimate of spacing, considering all SKB sites, is 700 m. However, this might still be too large because of the possible existence of additional unidentified fracture zones. "

CONCLUSION

Although, borehole data only exist for the upper few hundreds of metres, it is reasonable to assume that gently dipping fracture zones exist frequently down to several km depth at the Finnsjön site and its surrounding region. The data presented above suggests a spacing of 600 m for these zones. This spacing was also partly applied in the SKB 91 (page 145) safety assessment for gently dipping zones.

Data from Finnsjön and SFR suggest that for gently dipping zones both a westerly (eg. Zone 2) and an easterly dip (eg. Zone H2 in SFR) of 10-20° should be assumed.

Thus, for the regional flow modelling and considering depths of several km, it is suggested that various patterns of gently dipping zones with the above mentioned geometrical characteristics should be assumed. These patterns are intersected by steeply dipping fracture zones of regional extent. Data regarding the location of these steeply dipping zones are available from published lineament analyses, e.g. Ahlbom et al., 1987.

REFERENCES

Ahlbom, K., Andersson P., Ekman L. and Tirén S., 1987: Characterization of fracture zones in the Brändan area, Finnsjön study site, central Sweden. SKB AR 88-09.

Ahlbom K., 1991: Typberg i Finnsjönområdet. SKB AR 91-15.

Carlsson, H., Carlsson L., and Tirén S., 1988: Occurrence of gently dipping fracture zones. SGAB IRAP 88306.

Lager, I., 1986. The Dannemora iron ore deposit. In Lundström I., and Papunen, H.: Mineral deposits of southwestern Finland and the Bergslagen Province, Sweden. Excursion guide nr 3.7. IAGOD Symposium, 1986. Sveriges Geologiska Undersökning, Serie C 61, pp 26-30.

Appendix C

Compilation of particle track diagrams

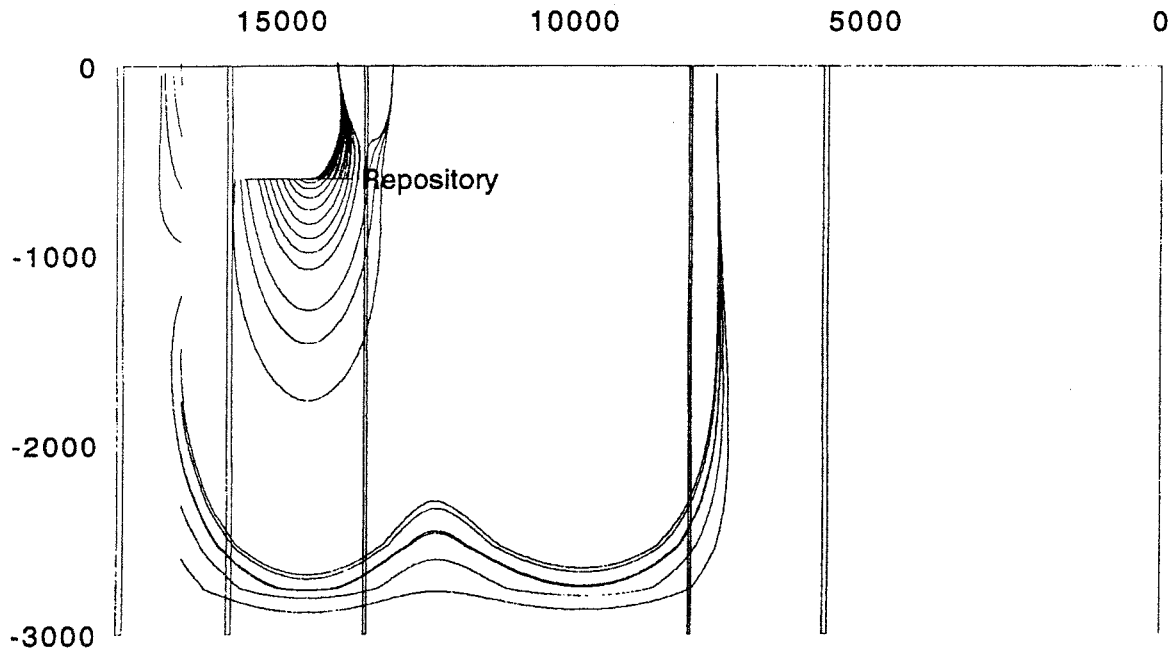

R1SDN

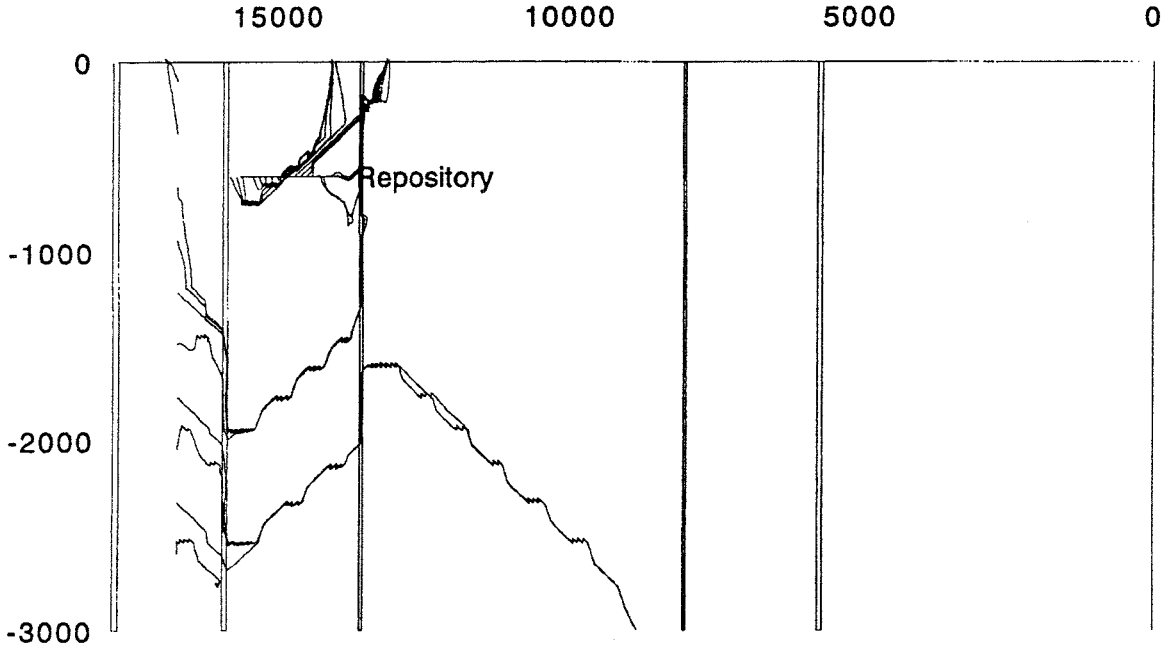

R1SDH1

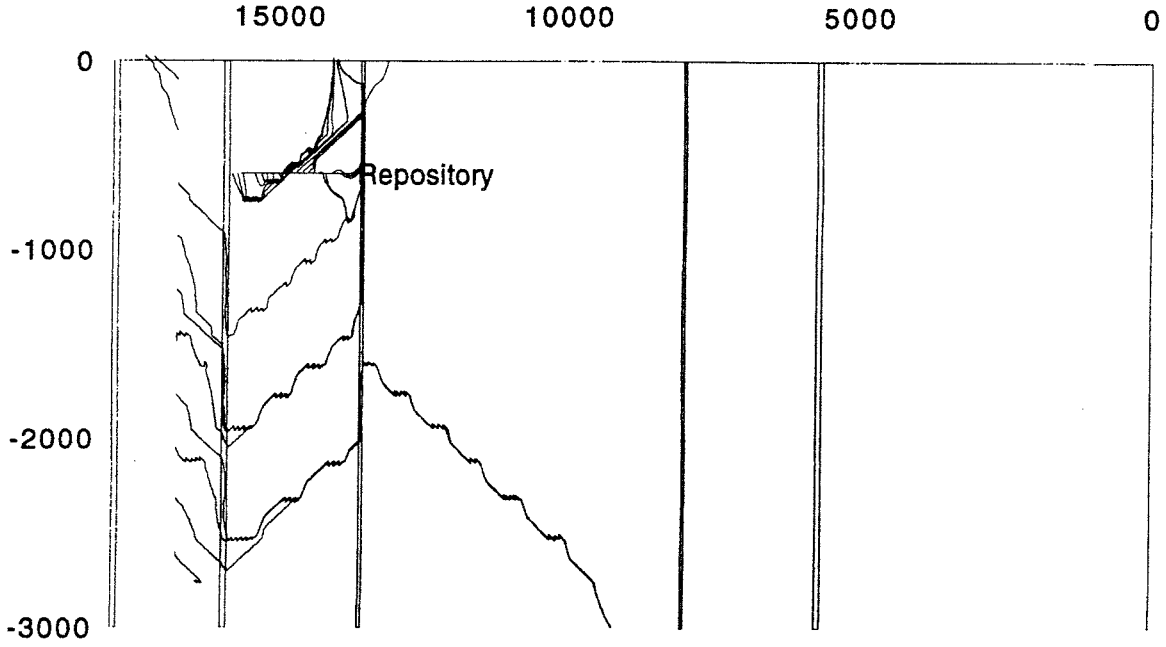

R1SDH2

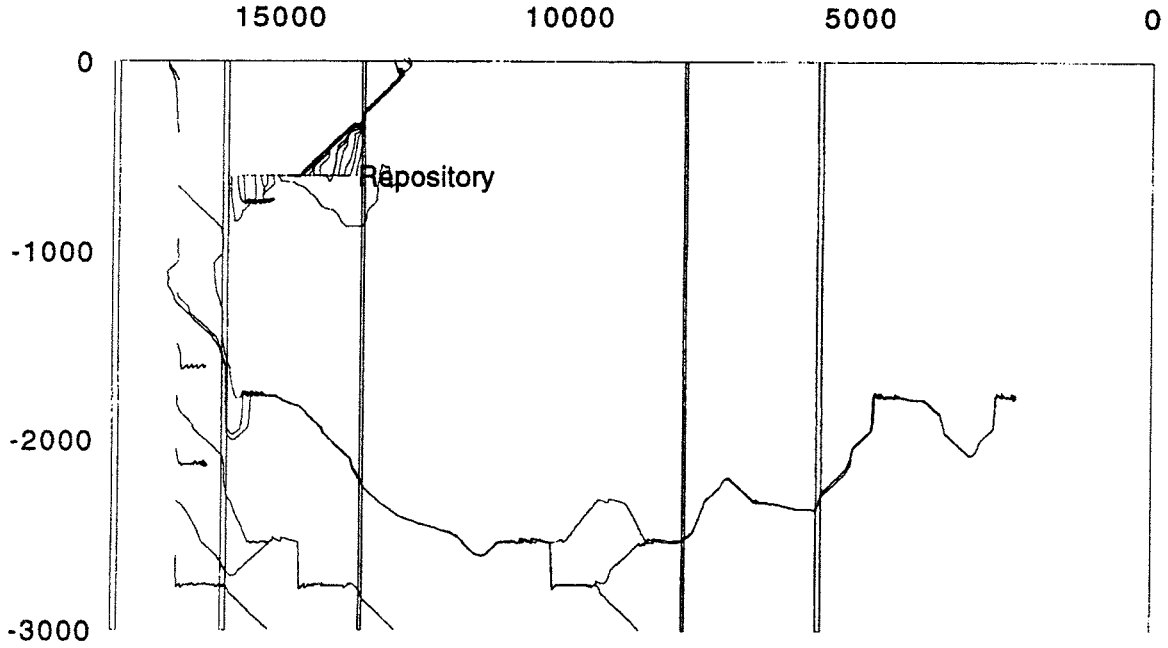

R1SDH3

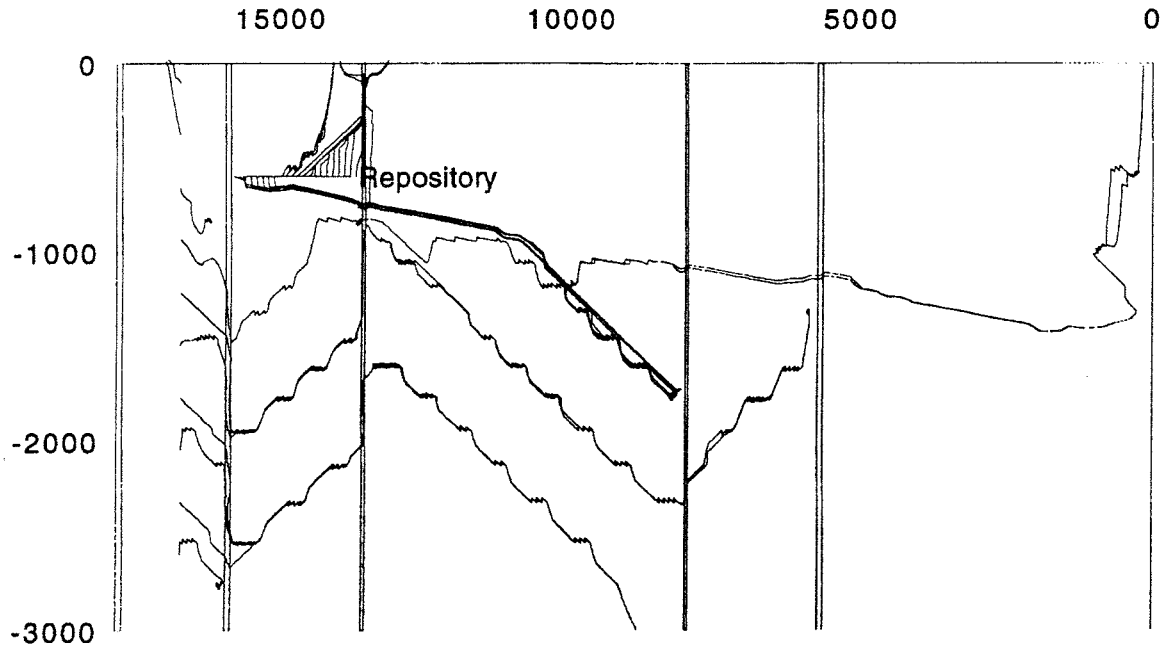

R1SDH4

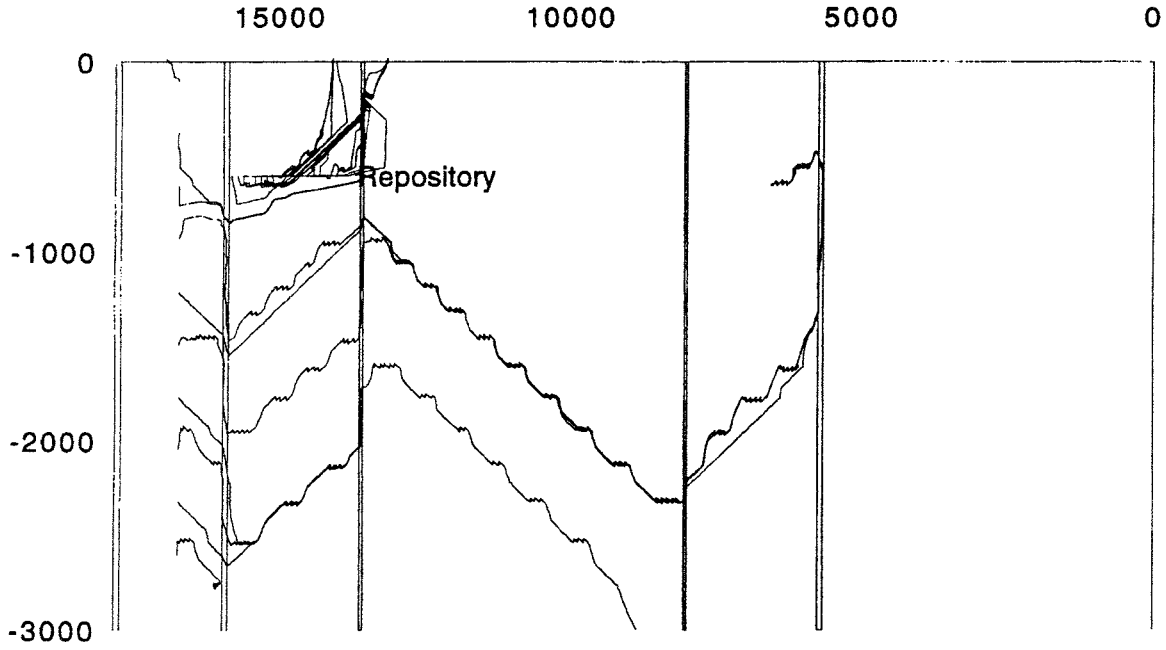

R1SDH5

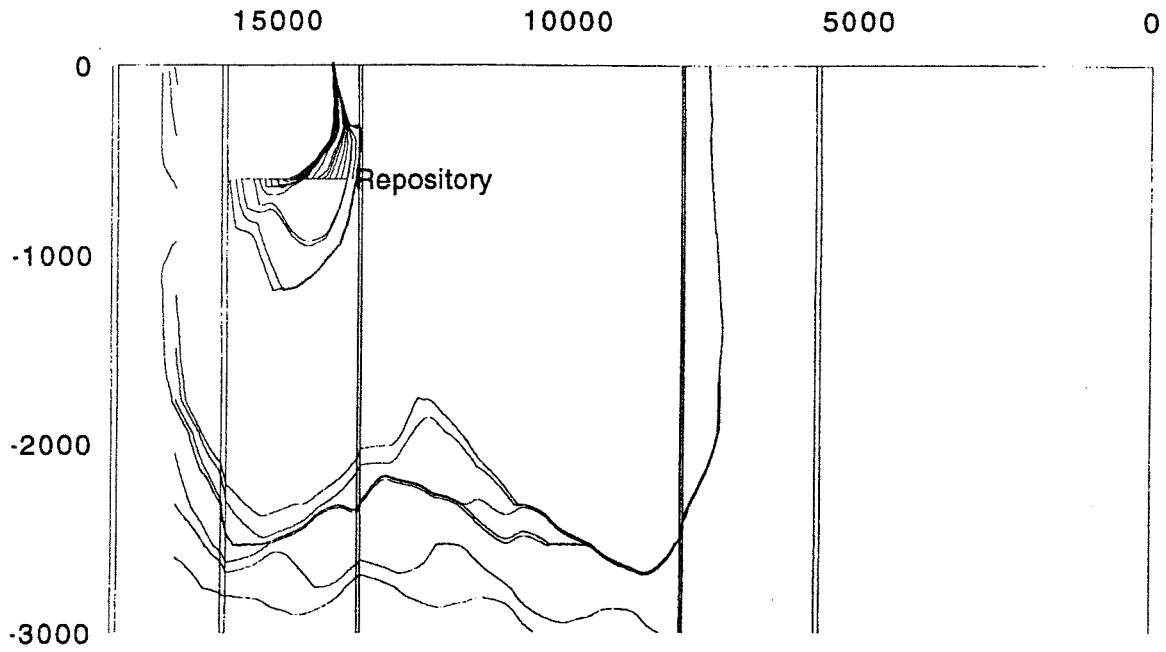

R1SDS1

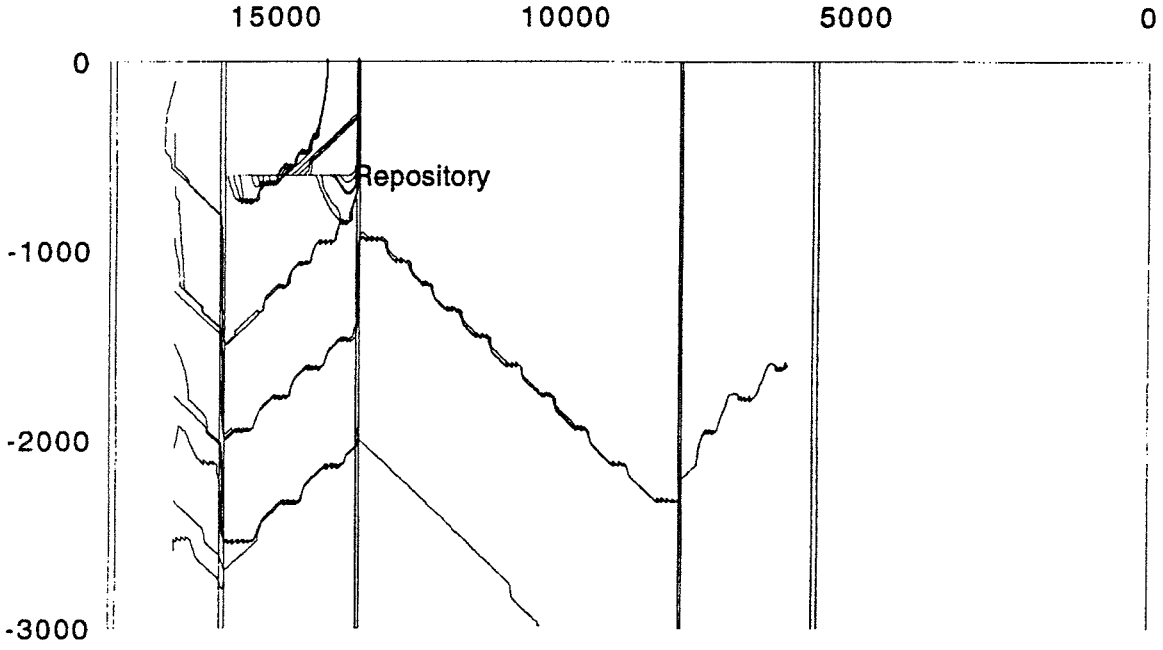

R1SNH1

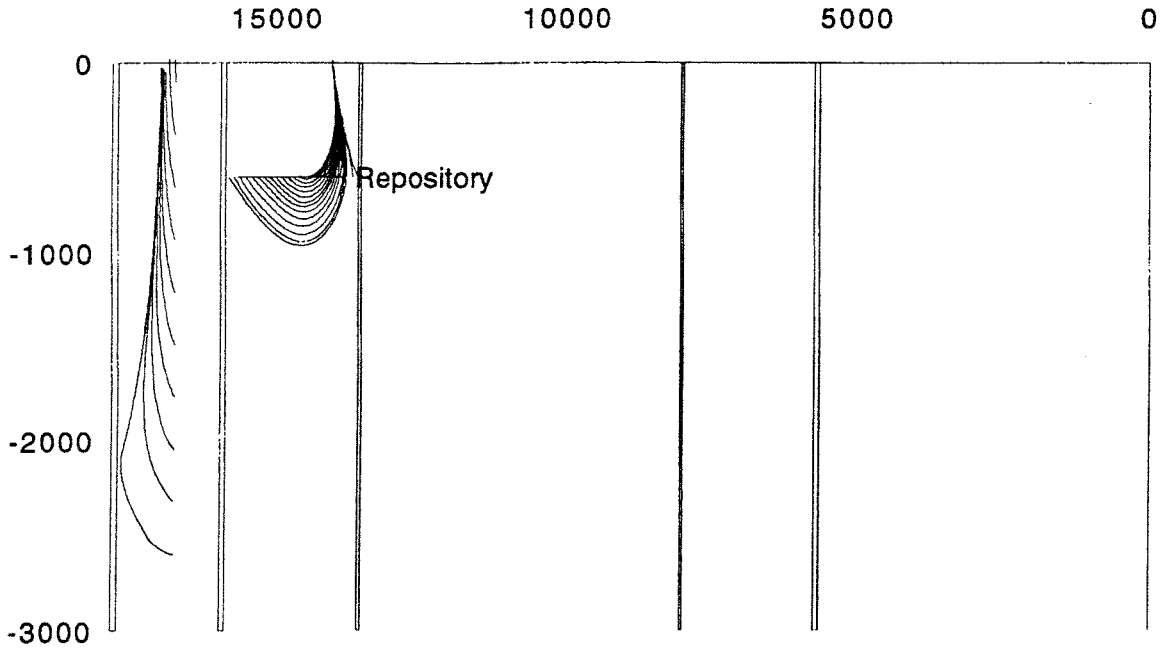

R1SDVV

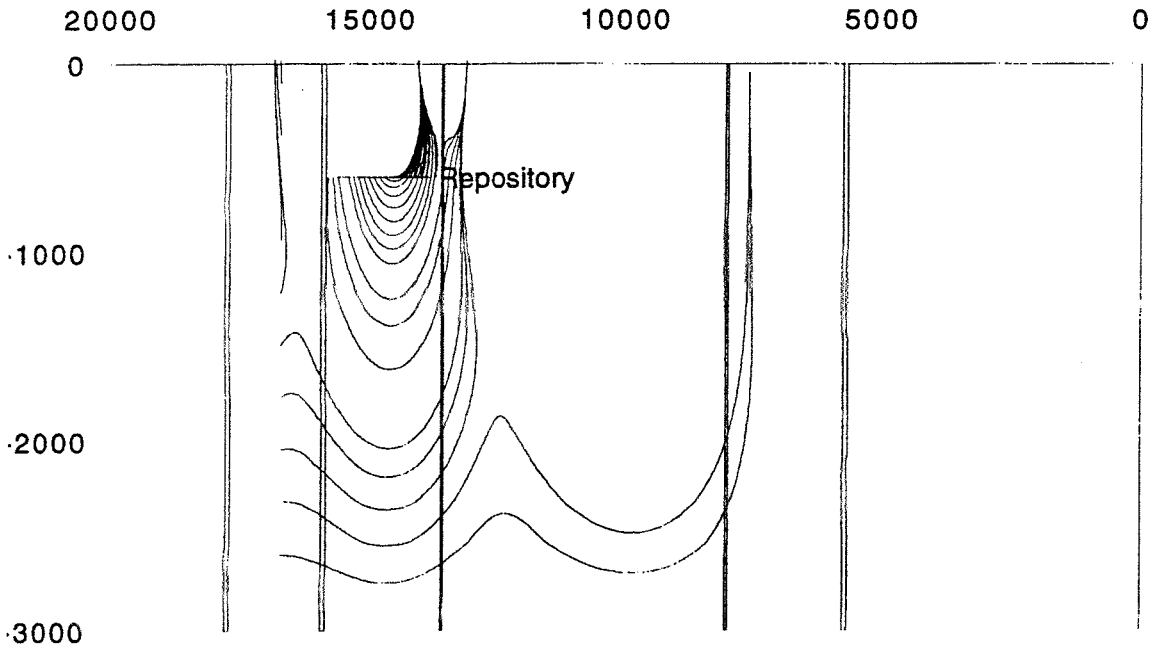

R2SDN

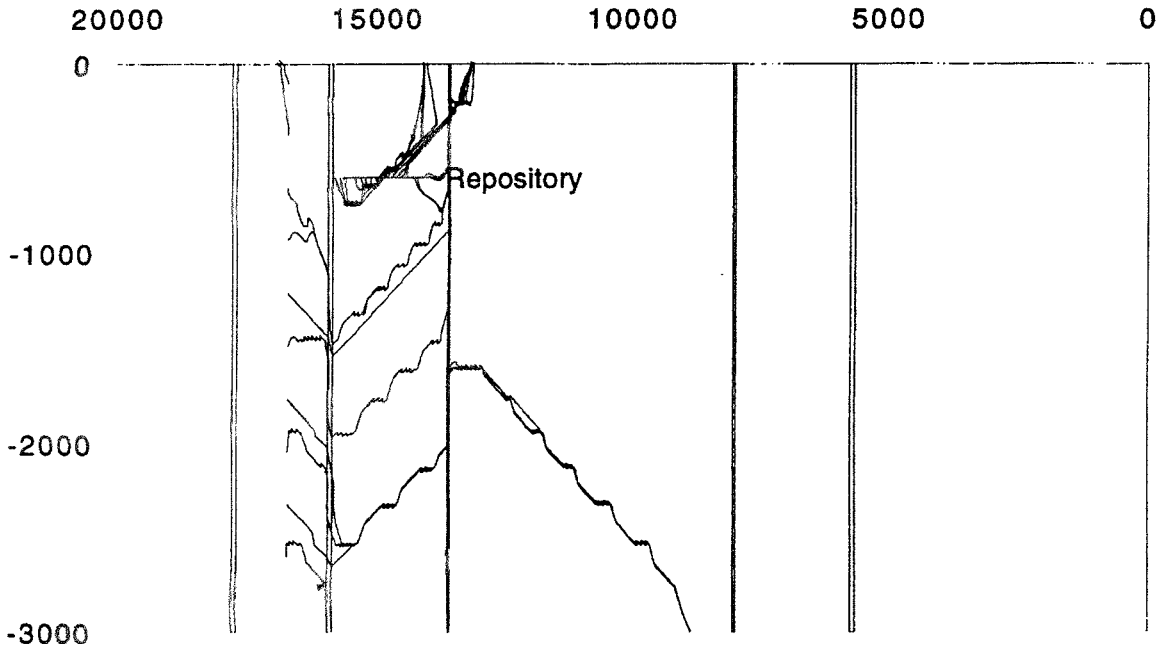

R2SDH1

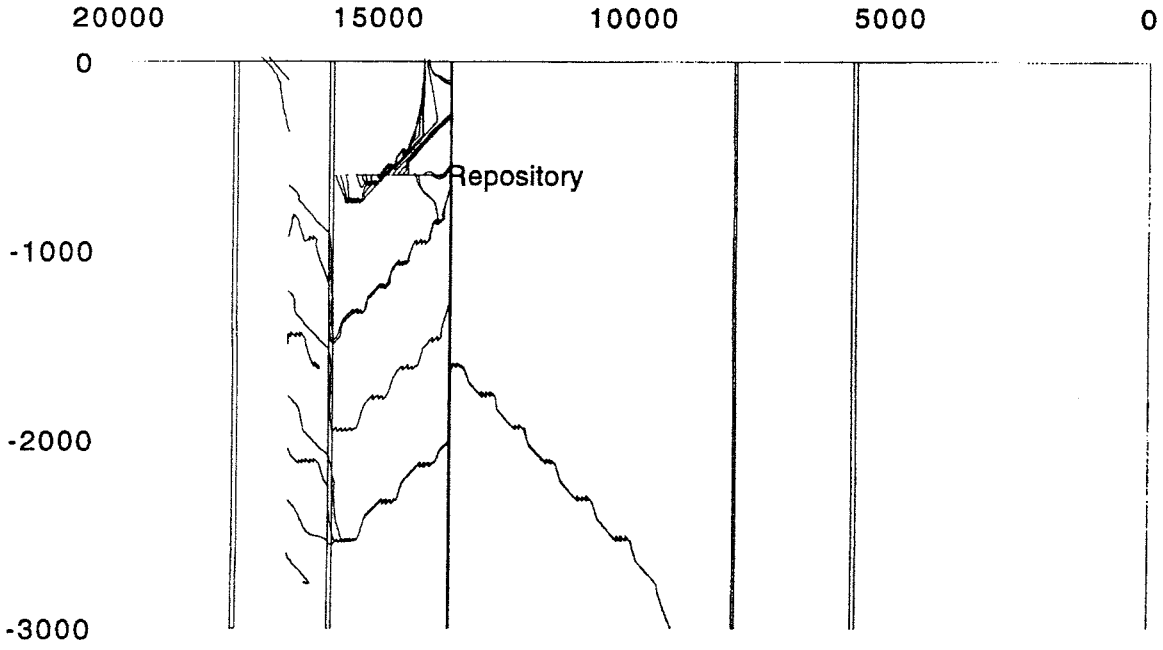

R2SDH2

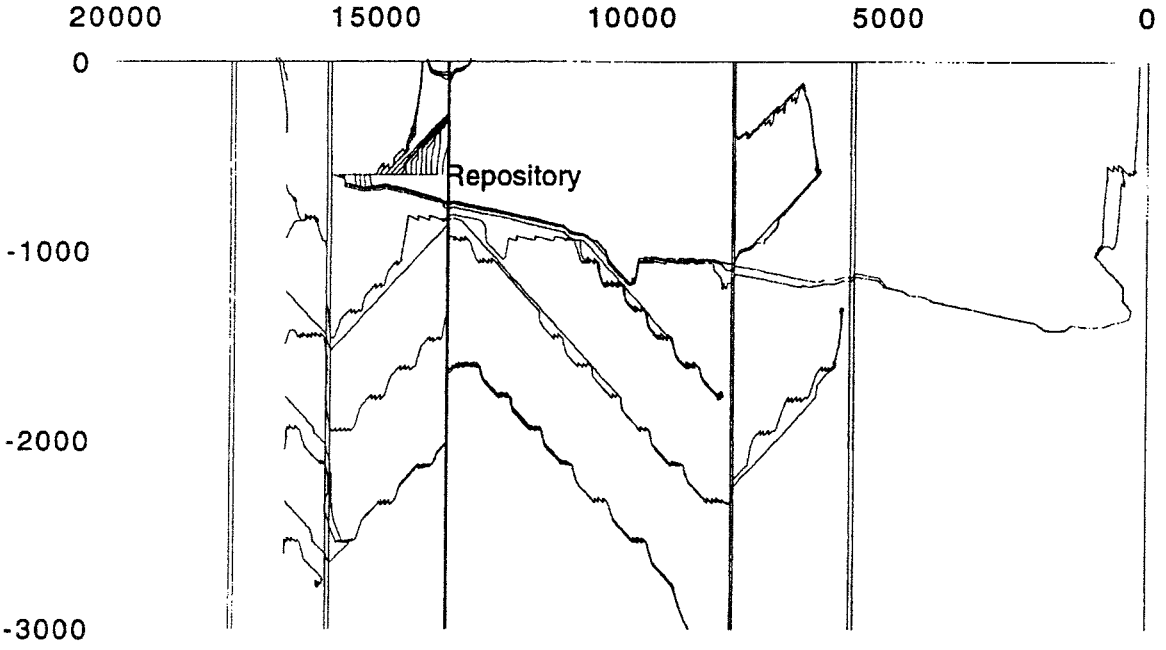

R2SDH4

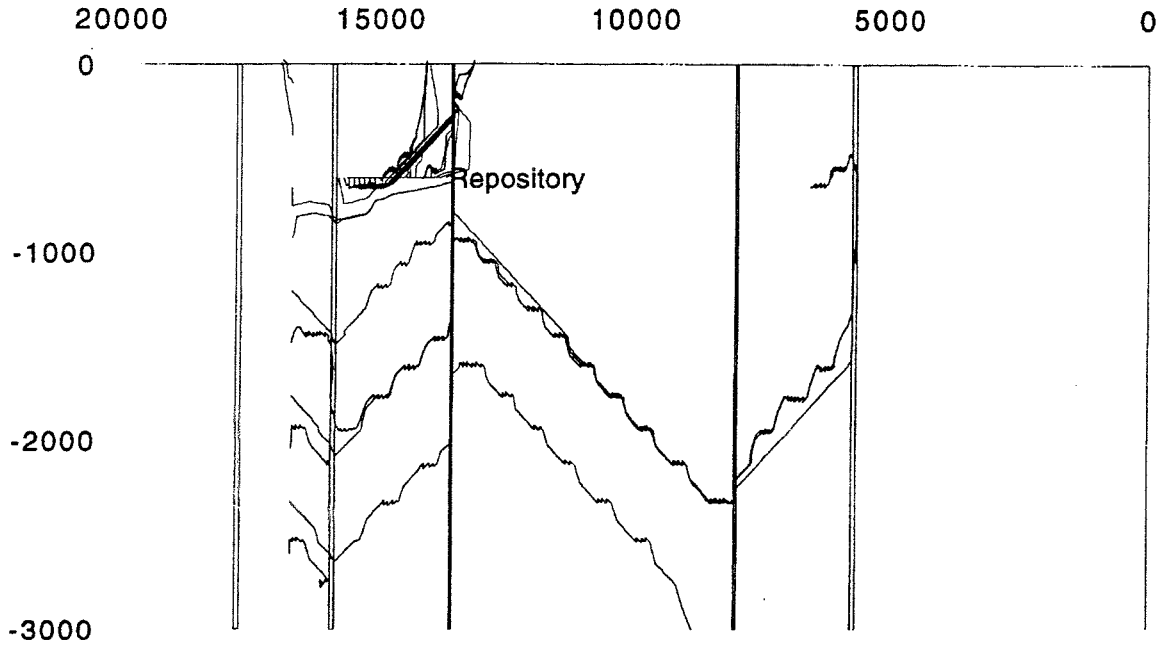

R2SDH5

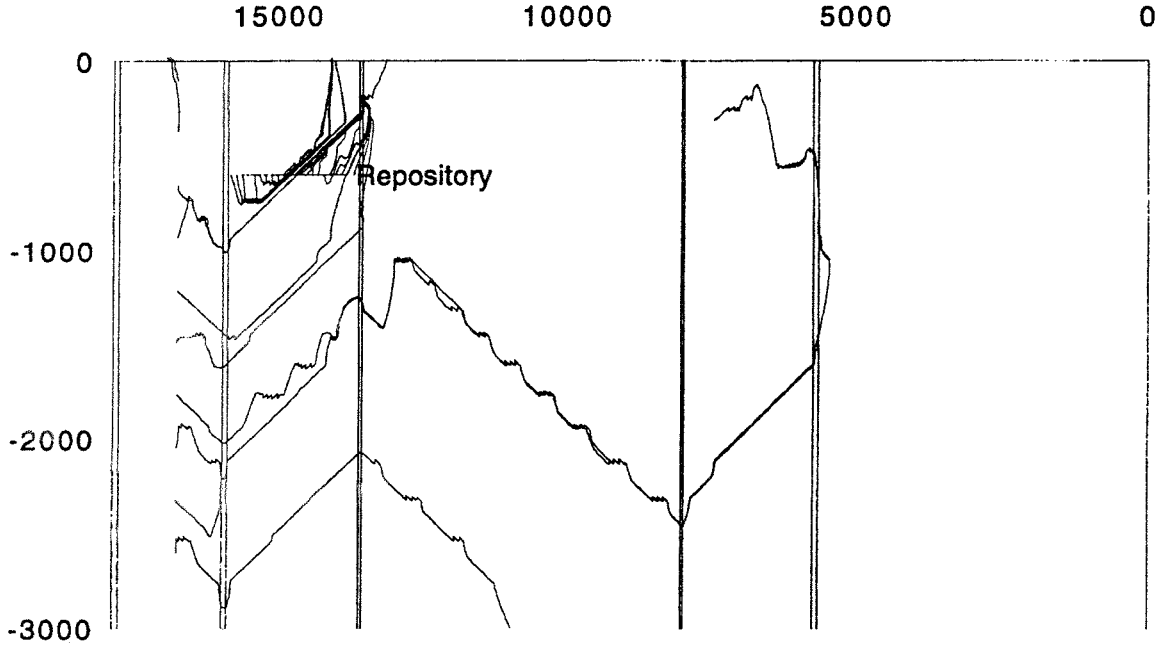

R2SDR1

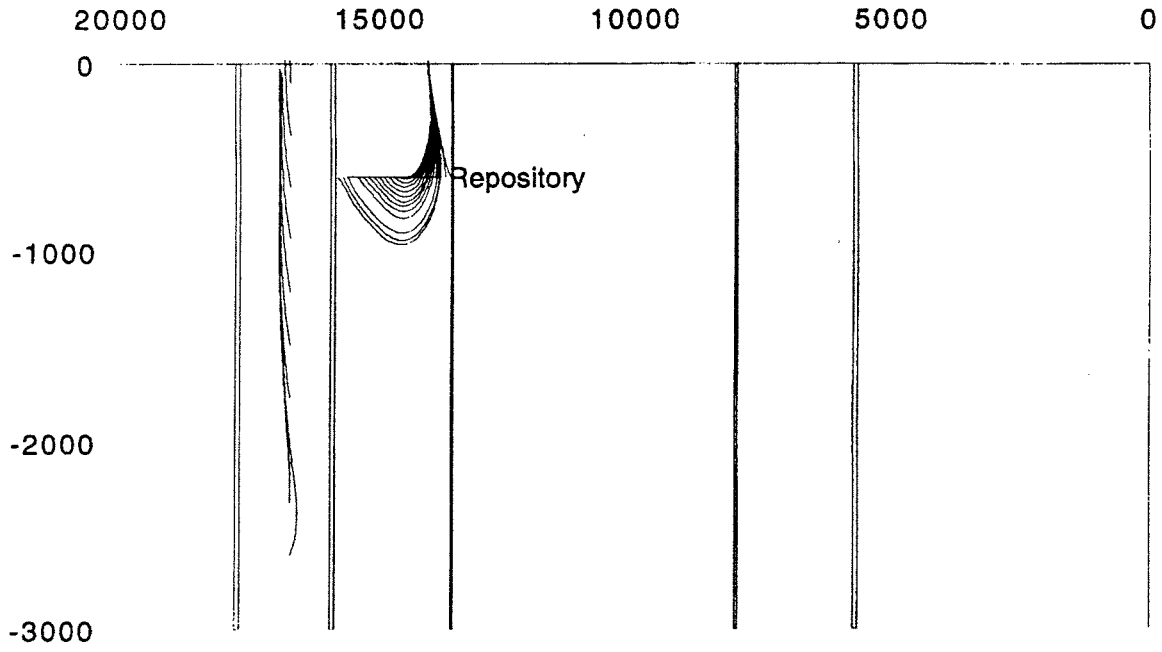

R2SDVV

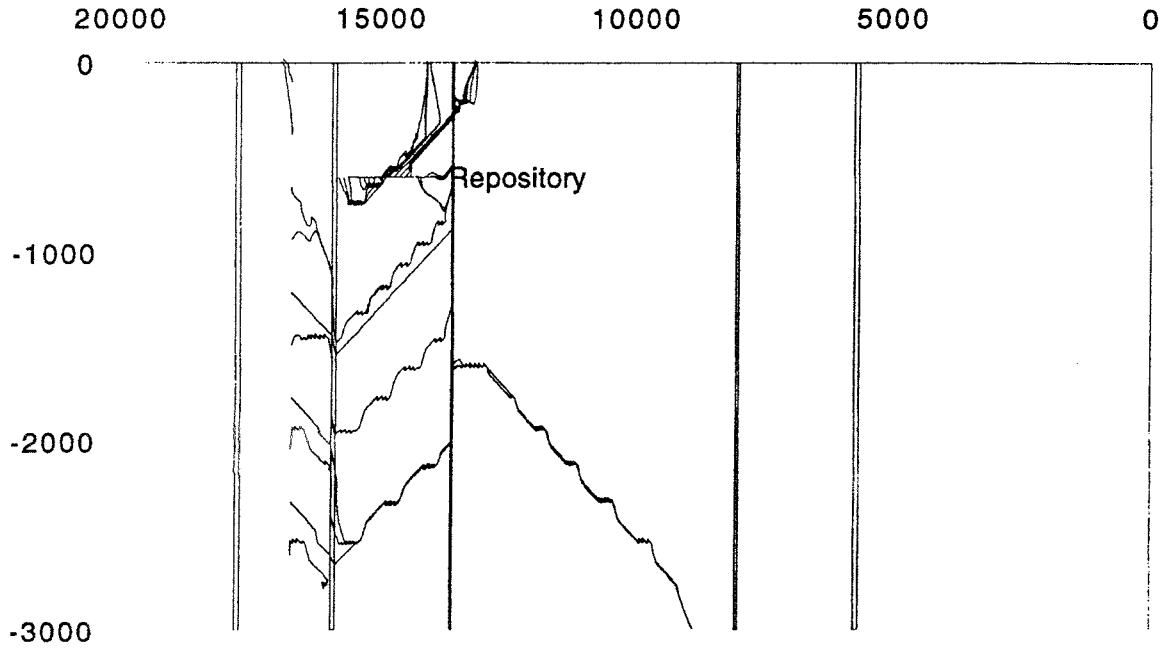

R3SDH1

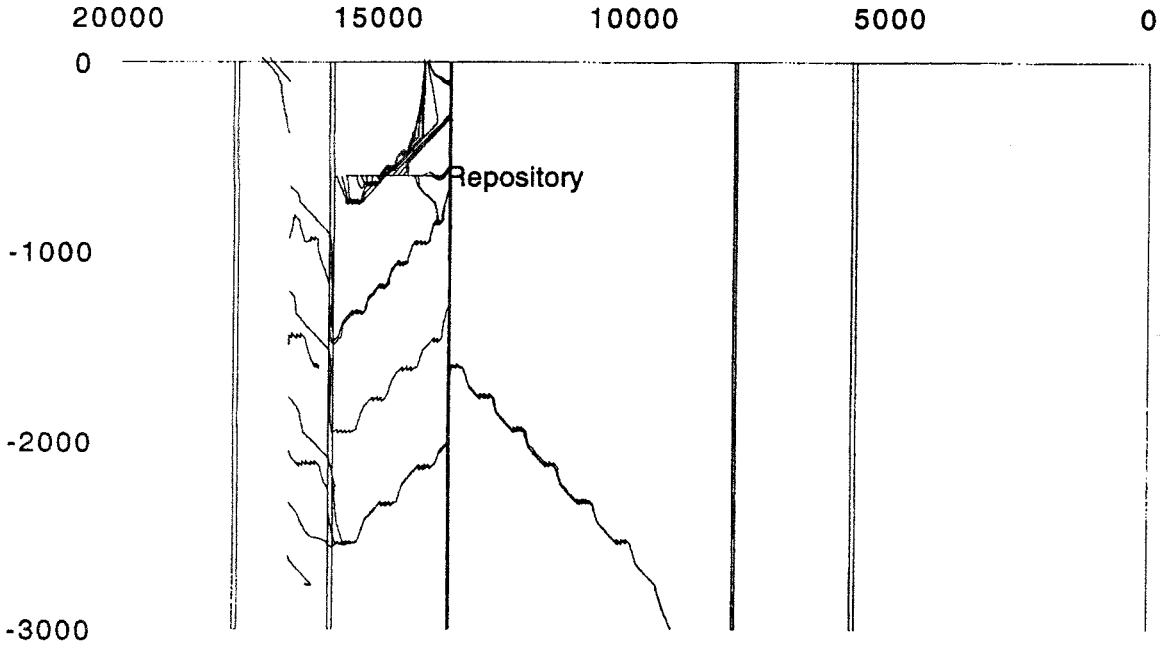

R3SDH2

List of SKB reports

Annual Reports

1977-78
TR 121
KBS Technical Reports 1 – 120
Summaries
Stockholm, May 1979

1979
TR 79-28
The KBS Annual Report 1979
KBS Technical Reports 79-01 – 79-27
Summaries
Stockholm, March 1980

1980
TR 80-26
The KBS Annual Report 1980
KBS Technical Reports 80-01 – 80-25
Summaries
Stockholm, March 1981

1981
TR 81-17
The KBS Annual Report 1981
KBS Technical Reports 81-01 – 81-16
Summaries
Stockholm, April 1982

1982
TR 82-28
The KBS Annual Report 1982
KBS Technical Reports 82-01 – 82-27
Summaries
Stockholm, July 1983

1983
TR 83-77
The KBS Annual Report 1983
KBS Technical Reports 83-01 – 83-76
Summaries
Stockholm, June 1984

1984
TR 85-01
Annual Research and Development Report 1984
Including Summaries of Technical Reports Issued during 1984. (Technical Reports 84-01 – 84-19)
Stockholm, June 1985

1985
TR 85-20
Annual Research and Development Report 1985
Including Summaries of Technical Reports Issued during 1985. (Technical Reports 85-01 – 85-19)
Stockholm, May 1986

1986
TR 86-31
SKB Annual Report 1986
Including Summaries of Technical Reports Issued during 1986
Stockholm, May 1987

1987
TR 87-33
SKB Annual Report 1987
Including Summaries of Technical Reports Issued during 1987
Stockholm, May 1988

1988
TR 88-32
SKB Annual Report 1988
Including Summaries of Technical Reports Issued during 1988
Stockholm, May 1989

1989
TR 89-40
SKB Annual Report 1989
Including Summaries of Technical Reports Issued during 1989
Stockholm, May 1990

1990
TR 90-46
SKB Annual Report 1990
Including Summaries of Technical Reports Issued during 1990
Stockholm, May 1991

1991
TR 91-64
SKB Annual Report 1991
Including Summaries of Technical Reports Issued during 1991
Stockholm, April 1992

1992
TR 92-46
SKB Annual Report 1992
Including Summaries of Technical Reports Issued during 1992
Stockholm, May 1993

Technical Reports
List of SKB Technical Reports 1993

TR 93-01
Stress redistribution and void growth in butt-welded canisters for spent nuclear fuel
B L Josefson[1], L Karlsson[2], H-Å Häggblad[2]
[1] Division of Solid Mechanics, Chalmers University of Technology, Göteborg, Sweden
[2] Division of Computer Aided Design, Luleå University of Technology, Luleå, Sweden
February 1993

TR 93-02
Hydrothermal field test with French candidate clay embedding steel heater in the Stripa mine
R Pusch[1], O Karnland[1], A Lajudie[2], J Lechelle[2], A Bouchet[3]
[1] Clay Technology AB, Sweden
[2] CEA, France
[3] Etude Recherche Materiaux (ERM), France
December 1992

TR 93-03
MX 80 clay exposed to high temperatures and gamma radiation
R Pusch[1], O Karnland[1], A Lajudie[2], A Decarreau[3],
[1] Clay Technology AB, Sweden
[2] CEA, France
[3] Univ. de Poitiers, France
December 1992

TR 93-04
Project on Alternative Systems Study (PASS).
Final report
October 1992

TR 93-05
Studies of natural analogues and geological systems.
Their importance to performance assessment.
Fredrik Brandberg[1], Bertil Grundfelt[1], Lars Olof Höglund[1], Fred Karlsson[2],
Kristina Skagius[1], John Smellie[3]
[1] KEMAKTA Konsult AB
[2] SKB
[3] Conterra AB
April 1993

TR 93-06
Mineralogy, geochemistry and petrophysics of red coloured granite adjacent to fractures
Thomas Eliasson
Chalmers University of Technology and University of Göteborg, Department of Geology, Göteborg, Sweden
March 1993

TR 93-07
Modelling the redox front movement in a KBS-3 nuclear waste repository
L Romero, L Moreno, I Neretnieks
Department of Chemical Engineering,
Royal Institute of Technology, Stockholm, Sweden
May 1993

TR 93-08
Äspö Hard Rock Laboratory
Annual Report 1992
SKB
April 1993

TR 93-09
Verification of the geostatistical inference code INFERENS, Version 1.1, and demonstration using data from Finnsjön
Joel Geier
Golder Geosystem AB, Uppsala
June 1993

TR 93-10
Mechanisms and consequences of creep in the nearfield rock of a KBS-3 repository
Roland Pusch, Harald Hökmark
Clay Technology AB, Lund, Sweden
December 1992

TR 93-11
Post-glacial faulting in the Lansjärv area, Northern Sweden.
Comments from the expert group on a field visit at the Molberget post-glacial fault area, 1991
Roy Stanfors (ed.)[1], Lars O Ericsson (ed.)[2]
[1] R S Consulting AB
[2] SKB
May 1993

TR 93-12
Possible strategies for geoscientific classification for high-level waste repository site selection
Lars Rosén, Gunnar Gustafson
Department of Geology, Chalmers University of Technology and University of Göteborg
June 1993

TR 93-13
A review of the seismotectonics of Sweden
Robert Muir Wood
EQE International Ltd, Warrington, Cheshire, England
April 1993

TR 93-14

Simulation of the European ice sheet through the last glacial cycle and prediction of future glaciation

G S Boulton, A Payne
Department of Geology and Geophysics,
Edinburgh University, Grant Insitute, Edinburgh,
United Kingdom

December 1992